HHS Public Access

Author manuscript

Cell Rep. Author manuscript; available in PMC 2025 November 05.

Published in final edited form as:

Cell Rep. 2025 October 28; 44(10): 116382. doi:10.1016/j.celrep.2025.116382.

HUWE1 stimulates mTORC1 activity by enhancing Rheb interaction with mTORC1 and supports *de novo* pyrimidine synthesis

Takayuki Ikeda[1,2], **Sungki Hong**[1], **Shota Yoshida**[1,8], **Swayam Prakash Srivastava**[1,8], **Abhiram Kunamneni**[1,8], **Yao Yao**[1], **Om Khuperkar**[1], **Venkatesha Basrur**[3], **Henry Kuang**[1,4], **Maureen Kachman**[5], **Abraham Raskind**[5], **Heidi Baum**[5], **Arya Joshi**[1,9], **Vinamra Swaroop**[1,9], **Aaron Thurman**[1,9], **Oliviamae Kopasz-Gemmen**[1,9], **Siddharth Kandukuri**[1,9], **F.N.U. Pradeepa**[1], **Hideto Yonekura**[2], **Jiandie D. Lin**[1,4], **Ken Inoki**[1,6,7,10,*]

[1] Life Sciences Institute, University of Michigan, 210 Washtenaw Avenue, Ann Arbor, MI 48109-2216, USA

[2] Department of Biochemistry, Kanazawa Medical University School of Medicine, 1-1 Daigaku, Uchinada, Kahoku-gun, Ishikawa 920-0293, Japan

[3] Department of Pathology, University of Michigan, 2800 Plymouth Road, Bldg. 35, Ann Arbor, MI 48109-2800, USA

[4] Department of Cell & Developmental Biology, University of Michigan Medical School, 109 Zina Pitcher Place, Ann Arbor, MI 48109-2200, USA

[5] Biomedical Research Core Facilities, University of Michigan, 1000 Wall Street, Ann Arbor, MI 48105-5714, USA

[6] Department of Molecular and Integrative Physiology, University of Michigan Medical School, 1137 E. Catherine St., Ann Arbor, MI 48109-5622, USA

[7] Department of Internal Medicine, University of Michigan Medical School, 1500 East Medical Center Drive, Ann Arbor, MI 48109-5368, USA

[8] These authors contributed equally

[9] These authors contributed equally

[10] Lead contact

SUMMARY

*Correspondence: inokik@umich.edu.

AUTHOR CONTRIBUTIONS

T.I., S.H., S.Y., A.K., S.P.S., Y.Y., and O.K. performed the experiments. H.K. performed AAV-TBG viral infection experiments. A.R., H.B., and M.K. measured the metabolites. V.B. performed mass spectrometry analyses. A.J. contributed to IF analyses. V.S., A.T., O.K.-G., and S.K. generated and maintained mouse colonies. F.N.U.P. performed hepatocyte isolation. H.Y. and J.D.L. helped with data analyses and discussions. T.I. and K.I. conceived the study and experimental design and wrote the manuscript.

DECLARATION OF INTERESTS

The authors declare no competing interests.

The mechanistic target of rapamycin complex 1 (mTORC1), a central regulator of cell growth, is activated by Rheb small GTPase. Our recent studies have demonstrated that polyubiquitinated Rheb enhances its interaction with mTORC1, resulting in the activation of mTORC1. Here, we demonstrate that the HECT, UBA, and WWE domain containing E3 ubiquitin protein ligase 1 (HUWE1), an E3 ubiquitin ligase, preferentially interacts with ubiquitinated Rheb and facilitates Rheb's binding to mTORC1 and its subsequent activation. The ablation of HUWE1 results in reduced ubiquitination of Rheb and decreased mTORC1 activity in cultured cells and mouse liver. HUWE1 is also necessary for Rheb to interact with carbamoyl-phosphate synthetase 2, aspartate transcarbamoylase, dihydroorotase (CAD), a key enzyme in pyrimidine biosynthesis, and for CAD activation through the activation of the mTORC1-S6K1 pathway. Moreover, HUWE1 maintains CAD expression by increasing its transcript in cells and liver tissues. Therefore, HUWE1 acts as a key organizer of the ubiquitinated Rheb complex, playing a vital role in enhancing mTORC1 activity and pyrimidine synthesis by increasing both CAD activity and expression.

In brief

Ikeda et al. identified that HUWE1 interacts with ubiquitinated Rheb, enhancing Rheb's binding to mTORC1 and CAD, leading to their activation. The study proposed that HUWE1 acts as a key organizer of the ubiquitinated Rheb complex, playing a vital role in enhancing mTORC1 activity and *de novo* pyrimidine synthesis.

Graphical Abstract

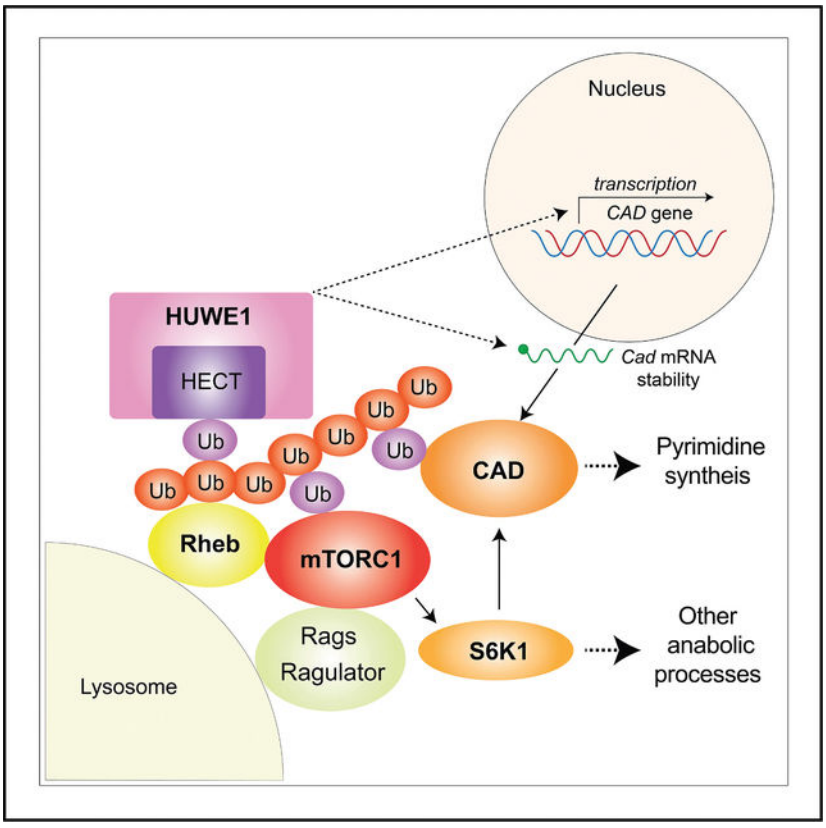

INTRODUCTION

The mechanistic target of rapamycin complex 1 (mTORC1) plays a central role in stimulating cellular anabolic processes, including the biogenesis of proteins, lipids, and nucleotides, which are essential for cell growth and proliferation.[1] In response to amino acids and growth factors, mTORC1 is primarily activated by two distinct Ras-related small guanosine triphosphatase (GTPases), Ras-related GTP-binding proteins (Rags), and Ras homolog enriched in brain (Rheb), on the lysosomal membrane.[2] While Rags recruit mTORC1 to the lysosomal membrane in response to amino acid availability, growth factors activate Rheb, which directly interacts with and stimulates mTORC1 on the lysosome.[3–7] For Rheb activation, growth factor-induced active protein kinase B (PKB/Akt) directly phosphorylates and inhibits the function of tuberous sclerosis complex 2 (TSC2), the GTPase-activating protein (GAP) for Rheb, by dislocating the TSC complex away from the lysosomal membrane, thereby providing a permissive condition to Rheb for its GTP-loading and activation.[8–17] In addition, recent studies demonstrated that the lysosomal localization of TSC2 is also reduced by amino acids.[18] However, guanine-nucleotide exchange factors (GEFs) for Rheb, which convert inactive Rheb to active Rheb, have not been convincingly demonstrated. Our recent studies have demonstrated that polyubiquitinated Rheb, induced by amino acids, facilitates the interaction between Rheb and mTORC1 and subsequent mTORC1 activation.[19,20] However, it has not been well understood what ubiquitin ligases contribute to Rheb polyubiquitination and its subsequent modifications, which support mTORC1 activation.

The homologous to E6-associated protein (E6-AP) carboxyl terminus (HECT), ubiquitin-associated (UBA), and tryptophan-tryptophan-glutamate (WWE) domain containing E3 ubiquitin protein ligase 1 (HUWE1) is a large E3 ubiquitin ligase containing multiple protein-protein interaction domains.[21] HUWE1 is known to ubiquitinate multiple lysine residues (e.g., K6, K48, and K63) to generate either polyubiquitin chains or branches on target proteins, leading to protein degradation or stabilization, respectively.[22,23] Known HUWE1-mediated degradation targets include both oncogenic proteins (e.g., c-Myc) and a tumor suppressor protein (p53), indicating that HUWE1 functions in both pro-apoptotic and anti-apoptotic pathways.[24–28] HUWE1 also inhibits autophagy induction by degrading WD repeat domain phosphoinositide-interacting protein 2 (WIPI2), a key protein that promotes autophagosome formation.[29] In contrast to its role in protein degradation, HUWE1 can generate K63-linked ubiquitin on c-Myc, facilitating its activation. Additionally, HUWE1 also forms K48 branches to K63 ubiquitin chains of tumor necrosis factor receptor-associated factor 6 (TRAF6), thereby amplifying nuclear factor κB (NF-κB) signaling.[23,24]

The carbamoyl-phosphate synthetase 2, aspartate transcarbamoylase, dihydroorotase (CAD) is a multifunctional enzyme that catalyzes the first three steps of *de novo* pyrimidine synthesis.[30] The enzyme activity of CAD is stimulated by S6K1-dependent phosphorylation, indicating that CAD is a key substrate of the mTORC1-S6K1 pathway.[31,32] A recent study also reported that Rheb and RhebL1 interact with CAD and stimulate its activity independently of mTORC1 activity.[33] The colocalization of CAD with RhebL1 on the lysosome membrane is diminished by a farnesyltransferase inhibitor that blocks membrane localization of RhebL1, suggesting that RhebL1 plays an important role in the lysosomal

localization of CAD. Inhibition of dehydroorotate dehydrogenase (DHODH) and uridine monophosphate synthetase (UMPS) in the *de novo* pyrimidine pathway showed little effect on cellular mTORC1 activity.[34,35] These observations suggest that CAD is a downstream effector of RhebL1 and Rheb and a substrate of the mTORC1-S6K1 pathway.

In this report, we identified that HUWE1 functions as a positive regulator for mTORC1 activation upstream of Rheb. The ablation of HUWE1 reduced levels of polyubiquitinated Rheb and mitigated cellular mTORC1 activity without affecting mTORC1 or TSC2 lysosomal localization and phosphorylation status of Akt and TSC2. Importantly, the ablation of HUWE1 diminishes the interaction of Rheb with mTOR and CAD. Furthermore, we found that HUWE1 also plays a key role in maintaining CAD expression. We propose that HUWE1 serves not only as a key organizer of the ubiquitinated Rheb-associated protein complex, which facilitates Rheb-dependent mTORC1/CAD activation, but also as an upstream positive regulator of CAD mRNA expression, thereby amplifying *de novo* pyrimidine synthesis.

RESULTS

Ubiquitinated Rheb displays a strong binding preference for HUWE1 and CAD

To identify Rheb ubiquitin ligases and possible Rheb GEFs, which have a strong binding preference for nucleotide-free small GTPases in general, we generated a nucleotide-free Rheb mutant in which the conserved glycine in the phosphate-binding loop was replaced with alanine (Figure 1A). An equivalent mutation of Ras (G15A) abrogates guanine nucleotide binding and promotes stable interaction with cdc25, a GEF for Ras.[36] As expected, the G18A Rheb mutant failed to bind guanine nucleotides, while the S16H and D60I mutants exclusively bound to GTP and GDP, respectively, as previously reported (Figure 1B).[37–40] The D60K mutant exhibited a largely diminished nucleotide binding capacity, with a small amount of remaining GDP (Figure 1B). Simultaneously, we observed that while all the Rhebs generated their polyubiquitinated forms mainly with K48-linked chains, which were migrated above 250 kDa, the Rheb D60I and G18A mutants displayed significantly higher levels of ubiquitination compared to those in the wild-type and S16H mutant (Figure 1C and S1A). The blockade of membrane tethering of Rheb by introducing a C181S mutation on the Rheb G18A mutant reduced the levels of ubiquitination, suggesting that membrane localization plays a role in supporting the ubiquitination of the Rheb G18A mutant, while cytoplasmic Rheb is also subjected to ubiquitination (Figure 1C). Thus, nucleotide-free Rheb G18A mutant would act as a potential bait to capture ubiquitin ligases for Rheb on the membrane and possible Rheb GEF proteins. To isolate such Rheb regulators, we performed protein purification using the Rheb G18A mutant and the Rheb S16H mutant as a control (Figure 1D). Silver staining demonstrated that two specific bands were predominantly co-immunoprecipitated (coIPed) with the Rheb G18A mutant. Through mass spectrometry analyses, we identified that these bands are HUWE1 and CAD. Among these Rheb mutants, G18A and D60I Rheb, which are highly ubiquitinated (Figure 1C), displayed a strong binding preference for endogenous HUWE1 and CAD (Figure 1E). Furthermore, as the blockade of membrane localization of Rheb reduced its ubiquitination (Figure 1C), levels of coIPed endogenous HUWE1 and CAD with the Rheb G18A/C181S

mutant were largely decreased compared to those with the Rheb G18A mutant (Figure 1F). These observations suggest that, rather than the nucleotide-binding status of Rheb, levels of ubiquitination or membrane localization may play a role in enhancing the binding of Rheb to HUWE1 and CAD. We also tested the interaction of endogenous Rheb with HUWE1 and CAD. While endogenous Rheb could coIP a very small amount of endogenous HUWE1 and CAD, levels of coIPed HUWE1 and CAD with endogenous Rheb were significantly increased when levels of ubiquitinated Rheb were maintained by N-ethylmaleimide (NEM), a deubiquitinase (DUB) inhibitor, during cell lysis and immunoprecipitation (Figures 1G and 1H). These results suggest that the preservation of the ubiquitinated form of Rheb maintains its binding affinity to both HUWE1 and CAD.

Similar to TSC2, both HUWE1 and CAD are primarily expressed in the cytoplasmic and membrane fractions (Figure S1B) and partially co-localize with Rheb in the perinuclear region (Figure S2A–S2E). Moreover, both HUWE1 and CAD could be detected in the purified lysosome, suggesting that certain levels of HUWE1 and CAD are expressed on the lysosome (Figure S2F, S2G, and S2H).

HUWE1 is required for Rheb to interact with CAD and mTOR

To understand the nature of HUWE1 and CAD interactions with Rheb, we first asked if HUWE1 interacts with CAD. HUWE1 coIPed CAD, and this interaction was modestly enhanced by growth factor/amino acid stimulation (Figure 2A). This result suggests that HUWE1 and CAD may be in the same complex with Rheb. To determine the key domains of CAD or HUWE1 that interact with Rheb, we generated various truncation mutants of CAD and HUWE1. CAD is a multifunctional enzyme that contains domains encoding glutaminase (GLN), carbamoyl phosphate synthetase (CPSase II), dihydroorotase (DHO), and aspartate transcarbamoylase (ATC) and catalyzes the first three steps of *de novo* pyrimidine biosynthesis (Figure 2B and also see Figure 6B). coIP experiments demonstrated that the Rheb G18A mutant effectively coIPed wild-type CAD and the mutants that contain the CPSase B domain (Figure 2B), which is consistent with previous observations.[33] On the other hand, the HECT domain, but not the UBA domain, of HUWE1 effectively coIPed Rheb G18A mutant (Figure 2C). The interaction of HUWE1 with Rheb G18A did not require HUWE1's catalytic activity, as the catalytically inactive HUWE1 C4341S mutant or the HECT domain with a C4341S mutation displayed an equivalent affinity to their wild-type proteins to interact with Rheb (Figure 2C). The HECT domain of HUWE1 was also coIPed with endogenous Rheb, and the levels of coIPed HECT domain were increased by NEM treatment (Figure 2D). Interestingly, both the full-length and the HECT domain of HUWE1 effectively coIPed the CPSase domains of CAD (Figures 2E and 2F). These data suggest that the HECT domain of HUWE1 or the CPSase domain of CAD may play a key role in assembling the HUWE1-Rheb-CAD complex.

To determine whether CAD is required for Rheb interaction with HUWE1, or vice versa, we depleted either CAD or HUWE1 using short hairpin RNA (shRNA)-mediated knockdown (KD) and monitored Rheb interactions with the other. While CAD KD had little effect on the interaction between Rheb G18A and HUWE1, HUWE1 KD largely diminished Rheb G18A interaction with CAD, indicating that HUWE1 is required for CAD to interact

with Rheb G18A mutant (Figure 3A). Importantly, HUWE1 KD but not CAD KD also disrupted the interaction between Rheb G18A mutant and mTOR, suggesting that HUWE1 may play a key role in the association between Rheb and mTOR (Figure 3A). Similar to the observations in HEK293T cells using Rheb G18A, CAD KD demonstrated little effect on growth factor/amino acid-induced interaction between endogenous Rheb and mTOR or TSC2 in mouse embryonic fibroblast (MEFs) (Figure 3B). Importantly, HUWE1 KD largely inhibited growth factor/amino acid-induced endogenous Rheb interaction with mTOR (Figure 3B). In contrast, HUWE1 KD had little effect on growth factor/amino acid-induced dissociation of TSC2 from Rheb (Figure 3B). These observations indicate that HUWE1 plays a key role in enhancing the interaction between Rheb and mTORC1 as well as CAD.

HUWE1 regulates Rheb ubiquitination

HUWE1 preferentially interacts with nucleotide-free or GDP-bound forms of Rheb mutants, which are highly ubiquitinated in the cells (Figures 1B–1E). We examined whether HUWE1 displays any GEF-like activity toward Rheb using purified HUWE1 and Rheb protein *in vitro* and found that HUWE1 did not exhibit a detectable guanine-nucleotide exchange activity for Rheb (Figure S3A).

Previous studies demonstrated several distinct ubiquitin ligases, including Siah1,[41] RNF152,[42] and DCAF1,[43] that ubiquitinate and degrade Rheb in response to nitric oxide, growth factor starvation, and glucose scarcity, respectively. Interestingly, we observed that while polyubiquitinated Rheb (Ub-Rheb) is gradually subjected to proteasomal and lysosomal degradation, Ub-Rheb forms a heteromultimer with non-ubiquitinated Rheb, facilitating their interaction with mTORC1 on the lysosome and leading to its subsequent activation. We recently identified that the CUL3-Rbx1-KLHL9 complex ubiquitinates Rheb to form “active” Ub-Rheb for mTORC1 activation,[20] whereas ataxin 3 (ATXN3) deubiquitinates Rheb and inhibits mTORC1 activation under amino acid-starved conditions.[19] To investigate if HUWE1 affects levels of Rheb ubiquitination, the effect of HUWE1 KD on wild-type and G18A Rheb ubiquitination was monitored in HEK293T. Under Rheb overexpressed conditions, while the effect was moderate, levels of total or K48-linked ubiquitination of both wild-type and G18A Rheb were consistently reduced in HUWE1 KD HEK293T cells (Figure 3C). Similarly, levels of polyubiquitinated endogenous Rheb were also reduced in HUWE1 KD or knockout (KO) HEK293T cells (Figure 3D and S3B). The trend of reduction in Ub-Rheb was also observed in HUWE1 KD HepG2 cells (Figure 3E). The ubiquitin ligase activity of HUWE1 is important for Rheb to interact with mTOR, as the reduced interaction of Rheb with mTOR in HUWE1 KD cells was partially restored by exogenous wild-type HUWE1 but not the C4341S HUWE1 mutant (Figure 3F). Since the ablation of HUWE1 did not eliminate Ub-Rheb, it suggests that HUWE1 is not a primary E3 ubiquitin ligase to generate the main polyubiquitinated form of Rheb; instead, it may act as a key ubiquitin modifier working with other ubiquitin ligases. The idea is also supported by the fact that HUWE1 showed a stronger binding preference for the Rheb mutants, which are highly ubiquitinated (Figures 1C–1F), or endogenous Rheb when its ubiquitination was maintained (Figures 1G and 1H). Together, these observations suggest that HUWE1 may play a key role in the interaction between Rheb and mTOR or CAD

through its ubiquitin ligase activity, likely by modifying (e.g., branching) the ubiquitinated form of Rheb (Figure 3G).

HUWE1 plays an important role in growth factor/amino acid-induced mTORC1 activation

Given the important role of HUWE1 in stimulating the interaction between Rheb and mTOR, we tested the effect of HUWE1 ablation on cellular mTORC1 activity in MEFs. Importantly, HUWE1 KD showed a substantial decrease in mTORC1 activity under normal cell culture conditions (basal) and in response to growth factor/amino acid stimulation (Figure 4A). Similar observations were also seen in HEK293T and HeLa cells (Figures S3C and S3D). Time course studies also demonstrated that the activation of mTORC1 was largely delayed and mitigated in HUWE1 KD MEFs (Figure 4B). While the initial induction of Akt, TSC2, or extracellular signal-regulated kinase (ERK) phosphorylation was slightly reduced 5 min after growth factor/amino acid stimulation in HUWE1 KD MEFs, it quickly recovered to similar or higher levels of phosphorylation in later time points compared to those in control cells (Figure 4B). Growth factor stimulation leads to the dissociation of TSC2 from the lysosome membrane in MEFs.[44] Consistent with the negligible effect of HUWE1 KD on TSC2 phosphorylation (Figure 4B) or TSC2 dissociation from Rheb (Figure 3B), insulin treatment sufficiently induced TSC2 dissociation from the lysosome in HUWE1 KD MEFs as in wild-type MEFs (Figure S3E). Despite these observations, the effect of HUWE1 KD on reducing mTORC1 activity was mitigated in cells lacking the TSC complex (Figure S3F). The observation suggests that the implication of HUWE1 in regulating the Rheb-mTORC1 activity requires an intact GDP-GTP cycle of Rheb, which is consistent with the observation that HUWE1 has a very weak affinity with GTP-bound Rheb, which is less ubiquitinated (Figures 1C and 1E). It is well known that HUWE1 ubiquitinates and degrades p53, a tumor suppressor that negatively regulates mTORC1 activity.[25,45] However, similar to the effects in wild-type MEFs, HUWE1 KD significantly inhibited growth factor-induced mTORC1 activity without affecting Akt phosphorylation in MEFs derived from p53 KO embryos (Figure 4C).[46] Together, these observations suggest that HUWE1 plays a crucial role in regulating mTORC1 activity independently of p53 function, acting downstream of Akt and TSC2. This is consistent with the observations that HUWE1 acts at the point of Rheb interaction with mTORC1 (Figures 3A and 3B). Consistently, HUWE1 KD also inhibited leucine-induced mTORC1 activation in MEFs (Figure 4D) without affecting amino acid-induced lysosomal mTOR localization (Figure 4E). Furthermore, the ablation of HUWE1 did not affect the levels of ubiquitination of Rag A and Rag C (Figure S3G) and effectively inhibited mTORC1 activity in HEK293T cells lacking nitrogen permease regulator 2-like protein (NPRL2), an essential catalytic component of GAP activity towards Rags-1 (GATOR1) (Figure 4F), supporting the notion that HUWE1 facilitates mTORC1 activation following its localization to the lysosome. To investigate if the ligase activity of HUWE1 plays an important role in the activation of mTORC1, we transiently introduced wild-type or the catalytically inactive HUWE1 C4341S mutant with HA-S6K1 as a reporter in HUWE1 KD HEK293T cells. Consistent with the observation that wild-type HUWE1, but not the C4341 HUWE1 mutant, restored Rheb interaction with mTOR in HUWE1 KD HEK293T cells (Figure 3F), the reduction of S6K1 phosphorylation in the HUWE1 KD cells was also restored by re-expressing wild-type HUWE1 but not by the HUWE1 C4341S mutant (Figure 4G). Notably, HUWE1 KD resulted in a slight but consistent decrease in

CAD expression (Figures 4A–4D). However, increasing CAD expression with exogenous CAD in HUWE1 KD cells did not influence the effects of wild-type HUWE1 or HUWE1 C4341S mutant on mTORC1 activity, indicating that the E3 ubiquitin ligase activity of HUWE1 contributes to the mechanism underlying HUWE1-dependent mTORC1 activation.

HUWE1 plays a key role in stimulating mTORC1 activation *in vivo*

To test the role of HUWE1 in the regulation of mTORC1 activity in a more physiologically relevant setting, hepatocyte-specific HUWE1 KO mice were generated. The *Huwe1*$^{f/y}$ male mice (*Huwe1* is an X-linked gene), as well as *Huwe1*$^{f/f}$ female mice, expressing *Alb-Cre* (*Huwe1 LKO* mice), grew normally and lived at least 2 years as wild-type mice (unpublished observations). Consistent with the observation in the cultured cells, 12-week-old male *Huwe1 LKO* mice fed normal chow displayed significantly reduced mTORC1 activity monitored by levels of phosphorylated S6 (S240/244), the sites directly phosphorylated by S6K1 in their liver tissues[47,48] (Figure 5A) without affecting Akt phosphorylation (S479) and hepatocyte nucleolus number (Figure S4A), supporting the idea that HUWE1 specifically enhances mTORC1 activity downstream of Akt. Immunoblot analyses also demonstrated that levels of S6K1 and 4EBP1 phosphorylation, two known direct mTORC1 substrates, and S6 phosphorylation were significantly decreased in the liver tissue lysates from *Huwe1 LKO* mice (*Huwe1*$^{-/y}$) compared to those from control mice (*Huwe1*$^{f/y}$) (Figure 5B).

Since Alb-Cre has been shown to start expressing in fetal liver tissues,[49] we also examined the effect of acute HUWE1 ablation on mTORC1 activity in adult liver tissues (12-week-old) using the adeno-associated viral-thyroxine binding globulin promoter-Cre recombinase (AAV-TBG-Cre) system.[50] Firstly, *Huwe1*$^{f/y}$ mice were injected with AAV-TBG-Cre or AAV-TBG-GFP (control) (Figure 5C). Secondly, the *Huwe1*$^{f/y}$ or control wild-type *Huwe1*$^{+/y}$ mice were injected with the AAV-TBG-Cre (Figure 5D). After 10 days of infection, levels of mTORC1 activity in the liver or kidney tissues were monitored. The expression of HUWE1 was effectively and specifically reduced in only the liver tissues of *Huwe1*$^{f/y}$ mice treated with AAV-TBG-Cre (Figures 5C, 5D, S4B, and S4C). Consistent with the observations in the Alb-Cre system (Figures 5A and 5B), mTORC1 activity in the liver tissues was reduced under both fasted and fed conditions in mice treated with the AAV-TBG-Cre but not with AAV-TBG-GFP (Figure 5C). Similarly, levels of mTORC1 activity in the liver tissues of *Huwe1*$^{f/y}$ mice treated with AAV-TBG-Cre were lower than those of control *Huwe1*$^{+/y}$ mice treated with the same AAV-TBG-Cre (Figure 5D). Together, these observations suggest that HUWE1 plays a crucial role in facilitating mTORC1 activity in liver tissues in response to food intake.

HUWE1 increases levels of CAD transcript and protein in liver tissues

The ablation of HUWE1 slightly but consistently decreased CAD expression in cultured cells (Figures 4A, 4B, 4D, and S3C). Similarly, CAD expression was drastically reduced in the liver tissues of *Huwe1 LKO* mice compared to that in *Huwe1*$^{f/y}$ control mice (Figure 6A). However, expression levels of other enzymes in the *de novo* pyrimidine synthesis pathway (Figure 6B), including DHODH or UMPS in *Huwe1 LKO* liver, remain unchanged (Figure 6C). Significant reduction of CAD protein expression was also observed in the liver

tissues in which the *Huwe1* gene was knocked out in the adult mice by the AAV-TBG-Cre (Figures 5C and 5D).

It has been reported that HUWE1 ubiquitinates c-MYC itself or ubiquitinates and degrades MIZ1, a suppressor of c-MYC, thereby enhancing c-MYC-dependent gene expression.[24,51] Furthermore, the transcription of the CAD gene is positively regulated by c-MYC.[52,53] To test if HUWE1 positively regulates CAD expression through its transcriptional activity, levels of CAD mRNA were monitored in HUWE1 KD HEK293T cells. As expected, HUWE1 KD reduced levels of not only CAD mRNA but also other c-MYC-target transcripts, such as CDK6, PPIE, and SLC16A1 (Figure S4D). Furthermore, the stability of CAD mRNA was not affected by the ablation of HUWE1 (Figure S4E), suggesting that HUWE1 enhances the transcriptional activity of the *CAD* gene in HEK293T cells, likely through c-Myc activation. We also tested whether the level of *Cad* gene expression was decreased in hepatocytes of *Huwe1 LKO* liver tissues. While levels of CAD mRNA were significantly reduced in *Huwe1 LKO* liver tissues compared to those of control *Huwe1*$^{f/y}$ liver tissues, as expected, we did not observe the reduction of other c-Myc-induced gene expressions, including DHODH, UMPS, and SLC16A1 in *Huwe1 LKO* liver tissues (Figure 6D and S4F).[54,55] Levels of LDHa and PKM2 mRNA, other known transcripts driven by c-Myc, were rather enhanced in *Huwe1 LKO* liver tissues compared to control *Huwe1*$^{f/y}$ liver tissues (Figure S4F).[56,57] These observations suggest that the mechanism underlying the reduction of CAD mRNA is not mainly due to the inhibition of c-Myc activity in *Huwe1 LKO* liver tissues. We observed that the stability of CAD mRNA was significantly decreased in the primary cultured hepatocytes from *Huwe1 LKO* liver tissues compared to the control hepatocytes (Figure 6E). These observations suggest that the mechanism by which CAD transcript is reduced in cells lacking HUWE1 expression differs between HEK293T cells and murine hepatocytes. Nevertheless, these observations suggest that HUWE1 plays a crucial role in maintaining CAD protein expression and its activity by increasing mRNA levels and enhancing mTORC1 activity, a key stimulator of CAD. To determine whether *de novo* pyrimidine synthesis is downregulated in the tissue lacking HUWE1 expression, we monitored the levels of metabolites, such as N-carbamoyl-L-aspartate (NCLA) and UMP (Figure 6B), in *Huwe1 LKO* and control liver tissues. As expected, levels of NCLA and UMP concentrations were slightly but consistently lower in the liver tissues of *Huwe1 LKO* mice compared to control mice (Figure 6F). Levels of lactate in the liver tissues, a metabolite indicating glycolysis status and hepatocyte functions, were not changed in *Huwe1 LKO* liver tissues.

Taken together, the data presented in this study propose a model in which HUWE1 functions as a key modulator of Ub-Rheb, acting as an mTORC1 activator by facilitating the interaction between mTORC1 and Rheb. Furthermore, our data indicate that HUWE1 also functions as a key player in supporting *de novo* pyrimidine synthesis by recruiting CAD into the Rheb-mTORC1 complex and maintaining CAD mRNA levels (Figure 6G).

DISCUSSION

In this study, we identified HUWE1 as a novel positive regulator of mTORC1 activity. HUWE1 plays a key role in the association of Rheb with mTOR and CAD, a known

substrate of Rheb and the mTORC1-S6K1 signaling.[31–33] Furthermore, HUWE1 is required to maintain the levels of CAD expression in both *in vitro* and *in vivo*. Given that HUWE1 shows a strong binding preference for inactive Rheb species, which are highly ubiquitinated when overexpressed, and display its positive role in activating mTORC1 activity, we suspected that HUWE1 might have a GEF-like activity toward Rheb. However, we failed to detect any nucleotide exchange activity of HUWE1 for Rheb *in vitro* (Figure S3A). Instead, we found that the E3 ligase activity of HUWE1 is required for HUWE1-induced mTORC1 activation (Figure 4G).

Our previous studies have indicated that the CUL3-Rbx1-KLHL9 ubiquitin ligase polyubiquitinates Rheb and supports its interaction with mTORC1 and subsequent mTORC1 activation on the lysosome.[19,20] The Rheb mutant with four lysine residues (K109/135/151/178A) displayed an impairment of its poly-ubiquitination, association with non-ubiquitinated Rheb and mTORC1, and the ability to enhance mTORC1 activity in response to amino acids and growth factors.[19,20] HUWE1-mediated protein ubiquitination contributes not only to the destabilization of target proteins through its K48-linked ubiquitination but also to the amplification of ubiquitin chain-mediated signal transduction. For instance, HUWE1 can activate c-Myc by catalyzing the assembly of K63-linked polyubiquitination chains, thereby inducing the transcriptional activation of a subset of c-Myc target genes.[24] In addition, HUWE1 also generates K48-linked branched ubiquitin chains on the K63 ubiquitin chains of TRAF6, leading to the amplification of the NF-κB signaling.[23] We propose that HUWE1 may act as a ubiquitin modifier of polyubiquitinated Rheb, likely forming branched chains that play a crucial role in amplifying the interaction between Rheb and mTORC1, leading to subsequent mTORC1 activation.

Interestingly, a recent study identified that Rheb also undergoes neddylation, a ubiquitin-like NEDD8 conjugation, through the ubiquitin-conjugating enzyme E2F (UBE2F)-sensitive to apoptosis gene (SAG) ligase on the same lysine residue that is subject to ubiquitination. The neddylation of Rheb positively regulates its function to stimulate mTORC1 activity.[19,58] These new observations also raise the possibility that, in addition to ubiquitin, HUWE1, which also acts as an E3 ligase for NEDD8,[59] may transfer NEDD8 to Rheb to confer Ub-Rheb resistance to immediate proteasome-mediated degradation, thereby supporting the interaction between Rheb and mTORC1 on the lysosome.

CAD is a known substrate of S6K1, and its activity is enhanced by S6K1-dependent phosphorylation.[31,32] A recent study postulated that GTP-bound active Rheb interacts with CAD and stimulates the CPS activity of CAD in a manner independent of mTORC1 activity.[33] Consistently, we also found that Rheb preferentially interacts with the CPSase domain of CAD. However, contrary to the model proposed in the previous paper, our observations suggest that the binding of Rheb to CAD is dependent on Rheb's ubiquitination status, regardless of its nucleotide-binding state. In support of this, the ablation of HUWE1 diminished the interaction of CAD with both wild-type and the highly ubiquitinated nucleotide-free Rheb mutant (Figures 3A and 3B). Given the critical role of mTORC1-S6K1 activity in stimulating CAD activity, it is conceivable that the formation of a multi-protein complex, including mTORC1 and CAD, induced by HUWE1-dependent Rheb

ubiquitination would be beneficial for amplifying mTORC1 signaling and expediting the transduction of mTORC1 signal to the *de novo* pyrimidine synthesis pathway.

Interestingly, we observed that ablation of HUWE1 also reduced CAD protein expression in cultured cells and tissues. Thus, HUWE1 stimulates not only the enzymatic activity of CAD through the activation of the mTORC1-S6K1 pathway but also CAD expression to support *de novo* pyrimidine synthesis. The mechanisms underlying HUWE1-induced CAD expression may differ across various cell types. For instance, HUWE1 increased CAD mRNA with little effect on its stability in HEK293T cells (Figure S4D and S4E), suggesting that HUWE1 may stimulate the transcription of the *CAD* gene. Transcriptional upregulation of the CAD gene, which contains the E-box sequence in its promoter, is known to be driven by the c-Myc transcription factor.[53,60] Notably, it has been reported that HUWE1-dependent ubiquitination of c-Myc or Miz1, a suppressive component of the c-Myc/Myc-associated factor X (MAX) complex, enhances E-box-associated c-Myc-target gene expression.[24,51] In fact, the ablation of HUWE1 in HEK293T cells suppressed the levels of many c-Myc-dependent transcripts bearing the E-box in their promoter (Figure S4D). Thus, it is conceivable that HUWE1 may enhance *CAD* gene expression through the activation of the c-Myc/MAX complex. Intriguingly, while the level of CAD mRNA was also significantly decreased in *HUWE1 LKO* liver tissues, we did not observe a reduction in the expressions of other known c-Myc-induced genes, such as *DHODH*, *LDHA*, and *SLC16A1*. Instead, we observed a decrease in CAD mRNA stability in HUWE1 KO primary hepatocytes. These observations indicate that HUWE1 maintains CAD transcripts through distinct mechanisms in HEK293T cells and murine hepatocytes.

HUWE1 has been shown to inhibit autophagy by degrading WIPI2, a key protein that is required for autophagosome formation in liver hepatocytes.[29,61] Interestingly, the study identified that mTORC1-dependent WIPI2 phosphorylation triggers HUWE1-dependent WIPI2 degradation.[62] However, the observations in this study suggest that HUWE1 may exert a broader role in inhibiting the processes of autophagy by supporting mTORC1 activity, which inhibits autophagy at several steps.[63–66] Finally, it has recently been reported that mice lacking HUWE1 in their hepatocytes (*Huwe1 LKO*) exhibited a significant reduction in lipid biogenesis and resistance to age- and high-fat diet-induced hepatic steatosis.[67] Interestingly, a recent study found that uridine 5'-triphosphate (UTP), a key metabolite derived from UMP, plays a crucial role in supporting pyruvate dehydrogenase activity and subsequent acetyl-CoA synthesis and fatty acid biogenesis, indicating another role of pyrimidine synthesis in lipid biogenesis.[68] Since the mTORC1-S6K1 pathway stimulates both lipid and pyrimidine biogenesis pathways through the activation of SERBPs and CAD, respectively,[31,32,69,70] it is conceivable that the reduction of mTORC1 activity and CAD expression in *Huwe1 LKO* liver tissues may contribute to protecting against aberrant lipid biogenesis and diet-induced non-alcoholic hepatic steatosis.

Limitations of the study

This study has not determined the key ubiquitin modifications of Rheb by HUWE1, which help assemble the Ub-Rheb complex consisting of Ub-Rheb, non-Ub Rheb, mTORC1, and CAD. We demonstrated that HUWE1 also plays a role in maintaining CAD expression

levels in cultured cells and liver tissues. However, the mechanisms underlying HUWE1-induced CAD expression differ and are dependent on the cell type. The detailed molecular mechanisms by which HUWE1 supports the levels of cellular CAD mRNA warrant future investigation.

RESOURCE AVAILABILITY

Lead contact

Requests for further information and resources should be directed to and will be fulfilled by the lead contact, Ken Inoki (inokik@umich.edu).

Materials availability

All unique/stable reagents generated in this study are available from the lead contact with a completed materials transfer agreement.

Data and code availability

- Raw western blotting and immunofluorescence (IF) data from Figures 1, 2, 3, 4, 5, and 6 and western blotting data from supplemental figures were deposited on Mendeley Data: https://data.mendeley.com/preview/snppdxjf2s, https://doi.org/10.17632/snppdxjf2s.1
- This paper does not report original code.
- Any additional information required to reanalyze the data reported in this paper is available from the lead contact upon request.

STAR★METHODS

EXPERIMENTAL MODEL AND STUDY PARTICIPANT DETAILS

Mouse model: *Huwe1*$^{f/f}$ (B6) and *Albumin Cre* (B6) mice were obtained from the Jackson Laboratory.[78] Congenital male HUWE1 liver-specific KO mice (*Huwe1*$^{f/y}$, *Alb-Cre*) were generated by crossing male *Albumin Cre* (B6) and female *Huwe1*$^{f/f}$ mice (*Huwe1* is a gene located on the X chromosome). Inducible male HUWE1 liver-specific KO mice were generated by infecting male *Huwe1*$^{f/y}$ mice (12-week-old) with AAV-TBG-Cre virus via the tail vein. In analyses of AAV-TBG-Cre-induced HUWE1 KO mice, after ten days of infection with control (AAV-TGB-GFP) and AAV-TBG-Cre, mice were starved for 16 h and fed for 5 h. The liver and kidney cortex tissues were homogenized with Triton X-100 lysis buffer (50 mM Tris-HCl [pH 7.5], 150 mM NaCl, 1% Triton X-100, 10% glycerol, 10 mM NaF, 10 mM pyrophosphate, 10 mM glycerophosphate, and a mixture of protease inhibitor (Roche)). All animal experiments were approved by the Institutional Animal Care and Research Advisory Committee at the University of Michigan.

Mammalian cell culture: HEK293T, HeLa, HepG2, wild-type mouse embryonic fibroblasts (MEFs), and p53$^{-/-}$ MEFs, p53$^{-/-}$ TSC2$^{-/-}$ MEFs (gifts from Dr. David Kwiatkowski, Brigham and Women's Hospital Boston, MA, USA) were cultured in DMEM (Thermo Fisher Scientific) with 10% fetal bovine serum (FBS, Corning) and 100

units/ml penicillin and 100 μg/mL streptomycin (Thermo Fisher Scientific). Primary mouse hepatocytes were cultured in Williams E (Thermo Fisher Scientific) with 5% FBS and 100 units/ml penicillin and 100 μg/mL streptomycin. All cell lines used in the study were regularly checked for mycoplasma.

METHOD DETAILS

Cell treatment, transfection, and fractionation: For growth factor/nutrient starvation, cells were incubated with HBSS (Hank's Balanced Salt Solution, Invitrogen) for the indicated times. For growth factor or nutrient starvation, cells were incubated with FBS-free or leucine (Leu)-free media (Crystalgen) for the indicated time, respectively. For stimulation of these, growth media, insulin (Sigma-Aldrich), or Leu (RPI Corp.) were added for the indicated times. Transfection was performed using Lipofectamine (Invitrogen). MEFs were fractionated into the cytoplasmic, membrane, and nuclear fractions using the Subcellular Protein Fractionation Kit for Cultured Cells (Pierce).

Primary hepatocyte isolation: Control (*Huwe1*$^{f/y}$) and *Huwe1 L KO* (*Huwe1*$^{-/y}$) liver tissues were perfused with HBSS and then with the collagenase-containing solution (HBSS with 1% BSA and 0.05% collagenase (Sigma-Aldrich)) for 10 min. Dispersed cells were resuspended and culture in the plate coated with 0.01% type I collagen (Sigma-Aldrich).

shRNAs, sgRNAs, lentivirus production: shRNAs or sgRNAs were cloned into the lentivirus plasmid pLKO.1-puro or Lenti-CRISPR v2, respectively. HEK293T cells were transfected with these plasmids with psPAX2 and pMD2.G to generate lentivirus carrying the shRNA or shRNA. Media containing lentivirus were collected and spun at 26,000 rpm for 100 min. Virus pellets were resuspended with Opti-MEM (Invitrogen) and stored at −80°C until use. Cells were infected for 24 h and selected with 2 μg/mL puromycin. 72 h post-infection, cells were harvested and processed for further analysis.

siRNA experiments: TriFECTa RNAi Kits were purchased from Integrated DNA Technologies (IDT). Two sequences for human HUWE1 were used: GCAGAUAAAUCUGAUCCUAAACCTG (hs.Ri.HUWE1.13.1) and GAUUCUGAAGCAAGUAGUCAAUCAG (hs.Ri.HUWE1.13.2). Non-targeting DsiRNA included in the kit was used as a negative control. siRNAs were pre-mixed with RNAiMAX (Invitrogen) for 10 min. HeLa cell suspension was seeded onto a 6-well plate at 2–3 × 10^5 cells/2.5 mL. siRNA/RNAiMAX mixture was added to the cells, and then the cells were incubated for 48 h.

Cell lysis and immunoprecipitation: Cells were harvested with NP40 lysis buffer (10 mM Tris-HCl [pH 7.5], 2 mM EDTA, 100 mM NaCl, 1% NP-40, 60 mM NaF, 10 mM pyrophosphate, 10 mM glycerophosphate, and a mixture of protease inhibitor (Roche)) for western blot analyses, CHAPS lysis buffer (40 mM HEPES [pH 7.5], 120 mM NaCl, 1 mM EDTA, 0.3% CHAPS, 50 mM NaF, 10 mM pyrophosphate, 30 mM glycerophosphate, and a mixture of protease inhibitor) for immunoprecipitation to assess protein-protein interaction, or RIPA lysis buffer (25 mM Tris-HCl [pH7.6], 50 mM NaCl, 1% NP-40, 1% sodium deoxycholate, 0.1% SDS, 50 mM NaF, 10 mM pyrophosphate,

10 mM glycerophosphate, and a mixture of protease inhibitor) for *in vivo* crosslinking samples. For immunoprecipitation using Flag-agarose beads, 15 μL of anti-FLAG M2 affinity gel (Sigma-Aldrich) was added and incubated with gentle rocking for 3 h at 4°C. For immunoprecipitation using the specific antibodies, 1 μg of antibody was added and incubated with gentle rocking for 3 h at 4°C. 15 μL of 50% slurry of protein G Sepharose (GE Healthcare) was added and incubated for an additional 1 h. Immunoprecipitates were washed with lysis buffer five times and then denatured at 100°C for 5 min in 1X SDS sample buffer.

Immunofluorescence staining of cultured cells: MEFs were plated on glass coverslips in a 6-well plate. Coverslips were rinsed with PBS and fixed with 4% paraformaldehyde (PFA) for 15 min and then permeabilized with 0.1% saponin and 2% BSA in PBS. After three washes with PBS, coverslips were incubated with the indicated primary antibodies in PBS containing 0.1% saponin and 2% BSA overnight at 4°C. The coverslips were washed 3 times with PBS and incubated with secondary antibodies (1:500) in 0.1% saponin/2% BSA for 2 h at room temperature. After 3 washes with PBS, the coverslips were mounted on the glass slides using Prolong Gold antifade reagent with DAPI (Invitrogen) and analyzed with a Leica TCS SP5 confocal microscope. The colocalization ratio was measured using the Fiji package of ImageJ (https://fiji.sc). Briefly, a binary image was created by Otsu's Threshold algorithm. The overlapped pixels were obtained by merging two binary images. The total pixel particles of each binary image and the merged image were measured by Analyze Particles. The ratio was calculated by the endogenous Rheb co-localized with endogenous HUWE1 or CAD to total endogenous Rheb, and the HUWE1 or CAD co-localized with Rheb to total HUWE1 or CAD.

Immunofluorescence staining of tissues: The liver tissues (right posterior segment VI) were fixed with PBS containing 4% PFA. The fixed tissues were embedded in paraffin and sectioned at 5 μm, and then subjected to immunofluorescence staining. Antibodies were used at the following dilutions: pS6 (1:400; Cell Signaling Technology); pAkt S473 (1:400; Cell Signaling Technology). Prolong Gold antifade reagent with DAPI (Invitrogen) was used for nucleus staining. The number of hepatocytes and the intensity of fluorescence signals were measured by ImageJ software. Briefly, the area was calculated with a standard measurement bar of 20 μm in each image. Vascular regions were eliminated from the area. Relative TRITC intensity (pS6 and pAkt) in the area was determined through ImageJ's measurement analysis tool. The DAPI channel was used to determine the number of hepatocyte nuclei by counting the particles of an area larger than 20 μm^2.

RT-qPCR: Cells were collected and lysed with TRIzol reagent (Invitrogen). Total RNA was purified using the RNeasy Mini Kit (QIAGEN). RT-qPCR was performed to determine the relative mRNA levels of human CAD, CDK6, PPIE, and SLC16A1 and murine CAD, DHODH, and UMPS using gene-specific primers (Supplemental information), the One Step TB Green PrimeScript PLUS RT-PCR kit (Takara), and the StepOnePlus Real-time PCR System (Applied Biosystems).

***In vivo* labeling:** GTP- and GDP-bound Rheb was determined by *in vivo* labeling with phosphorus-32 (^{32}P) radionucleotide as described previously.[10,38] Briefly, cells were washed once and incubated with phosphate-free DMEM (Invitrogen) for 90 min and incubated with phosphate-free DMEM containing 10% dialyzed FBS and 25 μCi ^{32}P-phosphate/mL for 4 h. Cells were lysed with cell lysis buffer (0.5% NP-40, 50 mM Tris-HCl [pH 7.5], 100 mM NaCl, 10 mM $MgCl_2$, 1 mM DTT, and a mixture of protease inhibitor) at 4°C for 30 s. The lysate was then centrifuged at 16,000 × g for 15 min at 4°C. To immunoprecipitate Flag-tagged Rheb, 10 μL of anti-FLAG M2 affinity gel was added to the supernatant and incubated with gentle rocking for 2 h at 4°C. The beads were washed with wash buffer 1 (50 mM Tris-HCl [pH 8.0], 500 mM NaCl, 5 mM $MgCl_2$, 1 mM DTT, 0.5% Triton X-100) three times at 4°C and then with wash buffer 2 (50 mM Tris-HCl [pH 8.0], 100 mM NaCl, 5 mM $MgCl_2$, 1 mM DTT, 0.1% Triton X-100) three times at 4°C. GTP and GDP nucleotides bound to Rheb were eluted with the elution buffer (2 mM EDTA, 0.2% SDS, 1 mM GDP, and 1 mM GTP) for 10 min at 68°C. Aliquots were spotted on PEI cellulose plates (Millipore) and resolved by thin-layer chromatography (TLC) with 0.75 M KH_2PO_4 (pH 3.4). Radionucleotides were detected with PhosphorImager (GE Healthcare) and quantified by ImageJ. The following formula is used to calculate the percentage of GTP: %GTP = (GTP/[(GDP x 1.5) + GTP]) × 100.

Protein identification by LC-Tandem MS: In-gel digestion: Immunoprecipitants with the indicated Flag-Rheb mutants were separated by SDS-PAGE and stained with Pierce Silver Stain for Mass Spec (ThermoFisher Scientific). Gel slice, including the specific bands co-IPed with Flag-Rheb G18A mutant, was destained with 30% methanol for 4 h. Upon reduction (10 mM DTT) and alklylation (65 mM 2-Chloroacetamide) of the cysteines, proteins were digested overnight with 500 ng of sequencing grade, modified trypsin (Promega) at 37°C. Peptides were extracted by incubating the gel with 150 μL of 50% acetonitrile/0.1% TFA for 30 min at room temperature. A second extraction with 150 μL of 100% acetonitrile/0.1% TFA was also performed. Both extracts were combined and dried in a vacufuge.

Liquid Chromatography and tandem mass spectrometry (LC-MS/MS): The resulting peptides were dissolved in 9 μL (for in-gel digest) or an appropriate volume of 0.1% formic acid/2% acetonitrile solution (to achieve ~500ng peptide/ul), and 2 μLs of the peptide solution were resolved on a nano-capillary reverse phase column (Acclaim PepMap C18, 2 μm, 50 cm, (ThermoFisher Scientific)) using a 0.1% formic acid/2% acetonitrile (Buffer A) and 0.1% formic acid/95% acetonitrile (Buffer B) gradient at 300 nL/min over a period of 90 min (2–25% buffer B in 45 min, 25–40% in 5 min, 40–90% in 5 min followed by holding at 90% buffer B for 5 min and reequilibration with Buffer A for 30 min). Eluent was directly introduced into the Orbitrap Fusion tribrid mass spectrometer (ThermoFisher Scientific) using an EasySpray source. MS1 scans were acquired at 120K resolution (AGC target = 1×10^6; max IT = 50 ms). Data-dependent collision-induced dissociation MS/MS spectra were acquired using the Top speed method (3 s) following each MS1 scan (NCE ~32%; AGC target 1×10^5; max IT 45 ms).

Database Search: Proteins were identified by searching the data against the UniProt Homo sapiens protein database appended with a standard contaminant protein list (ftp://

ftp.thegpm.org/fasta/cRAP) using Proteome Discoverer (v2.0, ThermoFisher Scientific). Search parameters included MS1 mass tolerance of 10 ppm and fragment tolerance of 0.1 Da; two missed cleavages were allowed; carbamidomethylation of cysteine, oxidation of methionine, and deamidation of asparagine and glutamine were considered as potential modifications. The FixedPSM validator of Proteome Discoverer was used to filter and retain high-quality proteins/peptides.

The protein samples were processed and analyzed at the Mass Spectrometry Facility of the Department of Pathology at the University of Michigan.

Metabolite measurement: Central Carbon Metabolism and Glycolysis/TCA sample preparation: Liver samples were removed from −80°C storage and maintained on wet ice throughout the processing steps. Samples were carefully resected and weighed to 30 mg +/− 3mg into a microtube containing stainless steel beads for tissue disruption, and the extraction solvent (1:1:1:1 = Methanol:Acetonitrile:Acetone:Water) was added at a ratio of 50 µL/mg of tissue. Tissue disruption was performed in a Precellys Evolution Touch homogenizer set to 0°C, 6200 rpm, for 3 cycles (20 s shake time and 30 s rest time per cycle.) After removal from the homogenizer, samples were incubated on ice for 10 min, vortexed to remix, then centrifuged at 14,000 RPM for 10 min at 4°C. 20 µL of the supernatant from each sample was removed to create a pooled sample for QC purposes. For both the pool and samples, 200 µL of the extract was transferred to an autosampler vial and dried under a gentle stream of nitrogen at room temperature. Dried samples were reconstituted in 100 µL of 80/20 water/methanol for LC-MS analysis. TCA and Central Carbon Metabolism LC-MS analysis: Samples were analyzed on an Ion Pairing LC-MS system consisting of an Agilent Infinity Lab II UPLC coupled with a 6545 QTOF mass spectrometer in negative ion mode, as previously described.[79] Semi-quantitative data for UMP and Lactate were obtained by manual integration using Profinder v8.00 (Agilent Technologies, Santa Clara, CA). Metabolites were identified by matching the retention time (±0.1 min), mass (±10 ppm), and isotope profile (peak height and spacing) to authentic standards run at the same time as the samples.

QUANTIFICATION AND STATISTICAL ANALYSIS

Statistical analysis: The significance of differences was determined using an unpaired two-tailed Student's t-test or one-way ANOVA. p values of less than 0.05 were considered statistically significant: *$p < 0.05$, **$p < 0.01$, ***$p < 0.001$, ****$p < 0.0001$.

Supplementary Material

Refer to Web version on PubMed Central for supplementary material.

ACKNOWLEDGMENTS

Metabolite measurements were performed by the University of Michigan Metabolomics Core. This study was supported by grants from the NIH (DK124709 and GM145631) and the Takeda Science Foundation.

REFERENCES

1. Ben-Sahra I, and Manning BD (2017). mTORC1 signaling and the metabolic control of cell growth. Curr. Opin. Cell Biol. 45, 72–82. 10.1016/j.ceb.2017.02.012. [PubMed: 28411448]
2. Bar-Peled L, and Sabatini DM (2014). Regulation of mTORC1 by amino acids. Trends Cell Biol. 24, 400–406. 10.1016/j.tcb.2014.03.003. [PubMed: 24698685]
3. Long X, Lin Y, Ortiz-Vega S, Yonezawa K, and Avruch J (2005). Rheb binds and regulates the mTOR kinase. Curr. Biol. 15, 702–713. 10.1016/j.cub.2005.02.053. [PubMed: 15854902]
4. Sancak Y, Thoreen CC, Peterson TR, Lindquist RA, Kang SA, Spooner E, Carr SA, and Sabatini DM (2007). PRAS40 is an insulin-regulated inhibitor of the mTORC1 protein kinase. Mol. Cell 25, 903–915. 10.1016/j.molcel.2007.03.003. [PubMed: 17386266]
5. Bar-Peled L, Chantranupong L, Cherniack AD, Chen WW, Ottina KA, Grabiner BC, Spear ED, Carter SL, Meyerson M, and Sabatini DM (2013). A Tumor suppressor complex with GAP activity for the Rag GTPases that signal amino acid sufficiency to mTORC1. Science 340, 1100–1106. 10.1126/science.1232044. [PubMed: 23723238]
6. Petit CS, Roczniak-Ferguson A, and Ferguson SM (2013). Recruitment of folliculin to lysosomes supports the amino acid-dependent activation of Rag GTPases. J. Cell Biol. 202, 1107–1122. 10.1083/jcb.201307084. [PubMed: 24081491]
7. Tsun ZY, Bar-Peled L, Chantranupong L, Zoncu R, Wang T, Kim C, Spooner E, and Sabatini DM (2013). The folliculin tumor suppressor is a GAP for the RagC/D GTPases that signal amino acid levels to mTORC1. Mol. Cell 52, 495–505. 10.1016/j.molcel.2013.09.016. [PubMed: 24095279]
8. Castro AF, Rebhun JF, Clark GJ, and Quilliam LA (2003). Rheb binds tuberous sclerosis complex 2 (TSC2) and promotes S6 kinase activation in a rapamycin- and farnesylation-dependent manner. J. Biol. Chem. 278, 32493–32496. 10.1074/jbc.C300226200. [PubMed: 12842888]
9. Garami A, Zwartkruis FJT, Nobukuni T, Joaquin M, Roccio M, Stocker H, Kozma SC, Hafen E, Bos JL, and Thomas G (2003). Insulin activation of Rheb, a mediator of mTOR/S6K/4E-BP signaling, is inhibited by TSC1 and 2. Mol. Cell 11, 1457–1466. [PubMed: 12820960]
10. Inoki K, Li Y, Xu T, and Guan KL (2003). Rheb GTPase is a direct target of TSC2 GAP activity and regulates mTOR signaling. Genes Dev. 17, 1829–1834. 10.1101/gad.1110003. [PubMed: 12869586]
11. Inoki K, Li Y, Zhu T, Wu J, and Guan KL (2002). TSC2 is phosphorylated and inhibited by Akt and suppresses mTOR signalling. Nat. Cell Biol. 4, 648–657. 10.1038/ncb839. [PubMed: 12172553]
12. Manning BD, Tee AR, Logsdon MN, Blenis J, and Cantley LC (2002). Identification of the tuberous sclerosis complex-2 tumor suppressor gene product tuberin as a target of the phosphoinositide 3-kinase/akt pathway. Mol. Cell 10, 151–162. [PubMed: 12150915]
13. Saucedo LJ, Gao X, Chiarelli DA, Li L, Pan D, and Edgar BA (2003). Rheb promotes cell growth as a component of the insulin/TOR signalling network. Nat. Cell Biol. 5, 566–571. 10.1038/ncb996. [PubMed: 12766776]
14. Stocker H, Radimerski T, Schindelholz B, Wittwer F, Belawat P, Daram P, Breuer S, Thomas G, and Hafen E (2003). Rheb is an essential regulator of S6K in controlling cell growth in Drosophila. Nat. Cell Biol. 5, 559–565. 10.1038/ncb995. [PubMed: 12766775]
15. Tee AR, Fingar DC, Manning BD, Kwiatkowski DJ, Cantley LC, and Blenis J (2002). Tuberous sclerosis complex-1 and -2 gene products function together to inhibit mammalian target of rapamycin (mTOR)-mediated downstream signaling. Proc. Natl. Acad. Sci. USA 99, 13571–13576. 10.1073/pnas.202476899. [PubMed: 12271141]
16. Tee AR, Manning BD, Roux PP, Cantley LC, and Blenis J (2003). Tuberous sclerosis complex gene products, Tuberin and Hamartin, control mTOR signaling by acting as a GTPase-activating protein complex toward Rheb. Curr. Biol. 13, 1259–1268. 10.1016/s0960-9822(03)00506-2. [PubMed: 12906785]
17. Zhang Y, Gao X, Saucedo LJ, Ru B, Edgar BA, and Pan D (2003). Rheb is a direct target of the tuberous sclerosis tumour suppressor proteins. Nat. Cell Biol. 5, 578–581. 10.1038/ncb999. [PubMed: 12771962]

18. Demetriades C, Doumpas N, and Teleman AA (2014). Regulation of TORC1 in response to amino acid starvation via lysosomal recruitment of TSC2. Cell 156, 786–799. 10.1016/j.cell.2014.01.024. [PubMed: 24529380]
19. Yao Y, Hong S, Ikeda T, Mori H, MacDougald OA, Nada S, Okada M, and Inoki K (2020). Amino Acids Enhance Polyubiquitination of Rheb and Its Binding to mTORC1 by Blocking Lysosomal ATXN3 Deubiquitinase Activity. Mol. Cell 80, 437–451.e6. 10.1016/j.molcel.2020.10.004. [PubMed: 33157014]
20. Yao Y, Hong S, Yoshida S, Swaroop V, Curtin B, and Inoki K (2025). The Cullin3-Rbx1-KLHL9 E3 ubiquitin ligase complex ubiquitinates Rheb and supports amino acid-induced mTORC1 activation. Cell Rep. 44, 115101. 10.1016/j.celrep.2024.115101. [PubMed: 39708321]
21. Bernassola F, Karin M, Ciechanover A, and Melino G (2008). The HECT family of E3 ubiquitin ligases: multiple players in cancer development. Cancer Cell 14, 10–21. 10.1016/j.ccr.2008.06.001. [PubMed: 18598940]
22. Michel MA, Swatek KN, Hospenthal MK, and Komander D (2017). Ubiquitin Linkage-Specific Affimers Reveal Insights into K6-Linked Ubiquitin Signaling. Mol. Cell 68, 233–246.e5. 10.1016/j.molcel.2017.08.020. [PubMed: 28943312]
23. Ohtake F, Saeki Y, Ishido S, Kanno J, and Tanaka K (2016). The K48-K63 Branched Ubiquitin Chain Regulates NF-kappaB Signaling. Mol. Cell 64, 251–266. 10.1016/j.molcel.2016.09.014. [PubMed: 27746020]
24. Adhikary S, Marinoni F, Hock A, Hulleman E, Popov N, Beier R, Bernard S, Quarto M, Capra M, Goettig S, et al. (2005). The ubiquitin ligase HectH9 regulates transcriptional activation by Myc and is essential for tumor cell proliferation. Cell 123, 409–421. 10.1016/j.cell.2005.08.016. [PubMed: 16269333]
25. Chen D, Kon N, Li M, Zhang W, Qin J, and Gu W (2005). ARF-BP1/Mule is a critical mediator of the ARF tumor suppressor. Cell 121, 1071–1083. 10.1016/j.cell.2005.03.037. [PubMed: 15989956]
26. Kon N, Zhong J, Qiang L, Accili D, and Gu W (2012). Inactivation of arf-bp1 induces p53 activation and diabetic phenotypes in mice. J. Biol. Chem. 287, 5102–5111. 10.1074/jbc.M111.322867. [PubMed: 22187431]
27. Zhao X, Heng JIT, Guardavaccaro D, Jiang R, Pagano M, Guillemot F, Iavarone A, and Lasorella A (2008). The HECT-domain ubiquitin ligase Huwe1 controls neural differentiation and proliferation by destabilizing the N-Myc oncoprotein. Nat. Cell Biol. 10, 643–653. 10.1038/ncb1727. [PubMed: 18488021]
28. Zhong Q, Gao W, Du F, and Wang X (2005). Mule/ARF-BP1, a BH3-only E3 ubiquitin ligase, catalyzes the polyubiquitination of Mcl-1 and regulates apoptosis. Cell 121, 1085–1095. 10.1016/j.cell.2005.06.009. [PubMed: 15989957]
29. Wan W, You Z, Zhou L, Xu Y, Peng C, Zhou T, Yi C, Shi Y, and Liu W (2018). mTORC1-Regulated and HUWE1-Mediated WIPI2 Degradation Controls Autophagy Flux. Mol. Cell 72, 303–315.e6. 10.1016/j.molcel.2018.09.017. [PubMed: 30340022]
30. Evans DR, and Guy HI (2004). Mammalian pyrimidine biosynthesis: fresh insights into an ancient pathway. J. Biol. Chem. 279, 33035–33038. 10.1074/jbc.R400007200. [PubMed: 15096496]
31. Ben-Sahra I, Howell JJ, Asara JM, and Manning BD (2013). Stimulation of de novo pyrimidine synthesis by growth signaling through mTOR and S6K1. Science 339, 1323–1328. 10.1126/science.1228792. [PubMed: 23429703]
32. Robitaille AM, Christen S, Shimobayashi M, Cornu M, Fava LL, Moes S, Prescianotto-Baschong C, Sauer U, Jenoe P, and Hall MN (2013). Quantitative phosphoproteomics reveal mTORC1 activates de novo pyrimidine synthesis. Science 339, 1320–1323. 10.1126/science.1228771. [PubMed: 23429704]
33. Sato T, Akasu H, Shimono W, Matsu C, Fujiwara Y, Shibagaki Y, Heard JJ, Tamanoi F, and Hattori S (2015). Rheb protein binds CAD (carbamoyl-phosphate synthetase 2, aspartate transcarbamoylase, and dihydroorotase) protein in a GTP- and effector domain-dependent manner and influences its cellular localization and carbamoyl-phosphate synthetase (CPSase) activity. J. Biol. Chem. 290, 1096–1105. 10.1074/jbc.M114.592402. [PubMed: 25422319]

34. Emmanuel N, Ragunathan S, Shan Q, Wang F, Giannakou A, Huser N, Jin G, Myers J, Abraham RT, and Unsal-Kacmaz K (2017). Purine Nucleotide Availability Regulates mTORC1 Activity through the Rheb GTPase. Cell Rep. 19, 2665–2680. 10.1016/j.celrep.2017.05.043. [PubMed: 28658616]
35. Hoxhaj G, Hughes-Hallett J, Timson RC, Ilagan E, Yuan M, Asara JM, Ben-Sahra I, and Manning BD (2017). The mTORC1 Signaling Network Senses Changes in Cellular Purine Nucleotide Levels. Cell Rep. 21, 1331–1346. 10.1016/j.celrep.2017.10.029. [PubMed: 29091770]
36. Chen SY, Huff SY, Lai CC, Der CJ, and Powers S (1994). Ras-15A protein shares highly similar dominant-negative biological properties with Ras-17N and forms a stable, guanine-nucleotide resistant complex with CDC25 exchange factor. Oncogene 9, 2691–2698. [PubMed: 8058333]
37. Heard JJ, Fong V, Bathaie SZ, and Tamanoi F (2014). Recent progress in the study of the Rheb family GTPases. Cell. Signal. 26, 1950–1957. 10.1016/j.cellsig.2014.05.011. [PubMed: 24863881]
38. Li Y, Inoki K, and Guan KL (2004). Biochemical and functional characterizations of small GTPase Rheb and TSC2 GAP activity. Mol. Cell Biol. 24, 7965–7975. 10.1128/MCB.24.18.7965-7975.2004. [PubMed: 15340059]
39. Tabancay AP Jr., Gau CL, Machado IMP, Uhlmann EJ, Gutmann DH, Guo L, and Tamanoi F (2003). Identification of dominant negative mutants of Rheb GTPase and their use to implicate the involvement of human Rheb in the activation of p70S6K. J. Biol. Chem. 278, 39921–39930. 10.1074/jbc.M306553200. [PubMed: 12869548]
40. Yan L, Findlay GM, Jones R, Procter J, Cao Y, and Lamb RF (2006). Hyperactivation of mammalian target of rapamycin (mTOR) signaling by a gain-of-function mutant of the Rheb GTPase. J. Biol. Chem. 281, 19793–19797. 10.1074/jbc.C600028200. [PubMed: 16728407]
41. Harraz MM, Tyagi R, Cortés P, and Snyder SH (2016). Antidepressant action of ketamine via mTOR is mediated by inhibition of nitrergic Rheb degradation. Mol. Psychiatry 21, 313–319. 10.1038/mp.2015.211. [PubMed: 26782056]
42. Deng L, Chen L, Zhao L, Xu Y, Peng X, Wang X, Ding L, Jin J, Teng H, Wang Y, et al. (2019). Ubiquitination of Rheb governs growth factor-induced mTORC1 activation. Cell Res. 29, 136–150. 10.1038/s41422-018-0120-9. [PubMed: 30514904]
43. Li M, Huang W, Zhang Y, Du Y, Zhao S, Wang L, Sun Y, Sha B, Yan J, Ma Y, et al. (2024). Glucose deprivation triggers DCAF1-mediated inactivation of Rheb-mTORC1 and promotes cancer cell survival. Cell Death Dis. 15, 409. 10.1038/s41419-024-06808-1. [PubMed: 38862475]
44. Menon S, Dibble CC, Talbott G, Hoxhaj G, Valvezan AJ, Takahashi H, Cantley LC, and Manning BD (2014). Spatial control of the TSC complex integrates insulin and nutrient regulation of mTORC1 at the lysosome. Cell 156, 771–785. 10.1016/j.cell.2013.11.049. [PubMed: 24529379]
45. Cui D, Qu R, Liu D, Xiong X, Liang T, and Zhao Y (2021). The Cross Talk Between p53 and mTOR Pathways in Response to Physiological and Genotoxic Stresses. Front. Cell Dev. Biol. 9, 775507. 10.3389/fcell.2021.775507. [PubMed: 34869377]
46. Zhang H, Cicchetti G, Onda H, Koon HB, Asrican K, Bajraszewski N, Vazquez F, Carpenter CL, and Kwiatkowski DJ (2003). Loss of Tsc1/Tsc2 activates mTOR and disrupts PI3K-Akt signaling through downregulation of PDGFR. J. Clin. Investig. 112, 1223–1233. 10.1172/JCI17222. [PubMed: 14561707]
47. Pende M, Um SH, Mieulet V, Sticker M, Goss VL, Mestan J, Mueller M, Fumagalli S, Kozma SC, and Thomas G (2004). S6K1 (−/−)/S6K2(−/−) mice exhibit perinatal lethality and rapamycin-sensitive 5'-terminal oligopyrimidine mRNA translation and reveal a mitogen-activated protein kinase-dependent S6 kinase pathway. Mol. Cell Biol. 24, 3112–3124. 10.1128/MCB.24.8.3112-3124.2004. [PubMed: 15060135]
48. Roux PP, Shahbazian D, Vu H, Holz MK, Cohen MS, Taunton J, Sonenberg N, and Blenis J (2007). RAS/ERK signaling promotes site-specific ribosomal protein S6 phosphorylation via RSK and stimulates cap-dependent translation. J. Biol. Chem. 282, 14056–14064. 10.1074/jbc.M700906200. [PubMed: 17360704]
49. Kellendonk C, Opherk C, Anlag K, Schütz G, and Tronche F (2000). Hepatocyte-specific expression of Cre recombinase. Genesis 26, 151–153. 10.1002/(sici)1526-968x(200002)26:2<151::aidgene17>3.0.co;2-e. [PubMed: 10686615]

50. Yan Z, Yan H, and Ou H (2012). Human thyroxine binding globulin (TBG) promoter directs efficient and sustaining transgene expression in liver-specific pattern. Gene 506, 289–294. 10.1016/j.gene.2012.07.009. [PubMed: 22820390]
51. Peter S, Bultinck J, Myant K, Jaenicke LA, Walz S, Müller J, Gmachl M, Treu M, Boehmelt G, Ade CP, et al. (2014). Tumor cell-specific inhibition of MYC function using small molecule inhibitors of the HUWE1 ubiquitin ligase. EMBO Mol. Med. 6, 1525–1541. 10.15252/emmm.201403927. [PubMed: 25253726]
52. Boyd KE, Wells J, Gutman J, Bartley SM, and Farnham PJ (1998). c-Myc target gene specificity is determined by a post-DNAbinding mechanism. Proc. Natl. Acad. Sci. USA 95, 13887–13892. 10.1073/pnas.95.23.13887. [PubMed: 9811896]
53. Bush A, Mateyak M, Dugan K, Obaya A, Adachi S, Sedivy J, and Cole M (1998). c-myc null cells misregulate cad and gadd45 but not other proposed c-Myc targets. Genes Dev. 12, 3797–3802. 10.1101/gad.12.24.3797. [PubMed: 9869632]
54. Zhang Q, Cui K, Kong Y, Yu J, Luo Z, Yang X, Gong L, Xie Y, Lin J, Liu C, et al. (2025). Targeting both the enzymatic and non-enzymatic functions of DHODH as a therapeutic vulnerability in c-Myc-driven cancer. Cell Rep. 44, 115327. 10.1016/j.celrep.2025.115327. [PubMed: 39977268]
55. Liu YC, Li F, Handler J, Huang CRL, Xiang Y, Neretti N, Sedivy JM, Zeller KI, and Dang CV (2008). Global regulation of nucleotide biosynthetic genes by c-Myc. PLoS One 3, e2722. 10.1371/journal.pone.0002722. [PubMed: 18628958]
56. He TL, Zhang YJ, Jiang H, Li XH, Zhu H, and Zheng KL (2015). The c-Myc-LDHA axis positively regulates aerobic glycolysis and promotes tumor progression in pancreatic cancer. Med. Oncol. 32, 187. 10.1007/s12032-015-0633-8. [PubMed: 26021472]
57. Mendez-Lucas A, Li X, Hu J, Che L, Song X, Jia J, Wang J, Xie C, Driscoll PC, Tschaharganeh DF, et al. (2017). Glucose Catabolism in Liver Tumors Induced by c-MYC Can Be Sustained by Various PKM1/PKM2 Ratios and Pyruvate Kinase Activities. Cancer Res. 77, 4355–4364. 10.1158/0008-5472.CAN-17-0498. [PubMed: 28630053]
58. Zhang F, Xiong X, Li Z, Wang H, Wang W, Zhao Y, and Sun Y (2025). RHEB neddylation by the UBE2F-SAG axis enhances mTORC1 activity and aggravates liver tumorigenesis. EMBO J. 44, 1185–1219. 10.1038/s44318-024-00353-5. [PubMed: 39762645]
59. Maghames CM, Lobato-Gil S, Perrin A, Trauchessec H, Rodriguez MS, Urbach S, Marin P, and Xirodimas DP (2018). NEDDylation promotes nuclear protein aggregation and protects the Ubiquitin Proteasome System upon proteotoxic stress. Nat. Commun. 9, 4376. 10.1038/s41467-018-06365-0. [PubMed: 30349034]
60. Miltenberger RJ, Sukow KA, and Farnham PJ (1995). An E-box-mediated increase in cad transcription at the G1/S-phase boundary is suppressed by inhibitory c-Myc mutants. Mol. Cell Biol. 15, 2527–2535. 10.1128/MCB.15.5.2527. [PubMed: 7739536]
61. Polson HEJ, de Lartigue J, Rigden DJ, Reedijk M, Urbé S, Clague MJ, and Tooze SA (2010). Mammalian Atg18 (WIPI2) localizes to omegasome-anchored phagophores and positively regulates LC3 lipidation. Autophagy 6, 506–522. 10.4161/auto.6.4.11863. [PubMed: 20505359]
62. Dooley HC, Razi M, Polson HEJ, Girardin SE, Wilson MI, and Tooze SA (2014). WIPI2 links LC3 conjugation with PI3P, autophagosome formation, and pathogen clearance by recruiting Atg12–5-16L1. Mol. Cell 55, 238–252. 10.1016/j.molcel.2014.05.021. [PubMed: 24954904]
63. Hosokawa N, Hara T, Kaizuka T, Kishi C, Takamura A, Miura Y, Iemura S.i., Natsume T, Takehana K, Yamada N, et al. (2009). Nutrient-dependent mTORC1 association with the ULK1-Atg13-FIP200 complex required for autophagy. Mol. Biol. Cell 20, 1981–1991. 10.1091/mbc.e08-12-1248. [PubMed: 19211835]
64. Kim YM, Jung CH, Seo M, Kim EK, Park JM, Bae SS, and Kim DH (2015). mTORC1 phosphorylates UVRAG to negatively regulate autophagosome and endosome maturation. Mol. Cell 57, 207–218. 10.1016/j.molcel.2014.11.013. [PubMed: 25533187]
65. Settembre C, Zoncu R, Medina DL, Vetrini F, Erdin S, Erdin S, Huynh T, Ferron M, Karsenty G, Vellard MC, et al. (2012). A lysosome-to-nucleus signalling mechanism senses and regulates the lysosome via mTOR and TFEB. EMBO J. 31, 1095–1108. 10.1038/emboj.2012.32. [PubMed: 22343943]

66. Roczniak-Ferguson A, Petit CS, Froehlich F, Qian S, Ky J, Angarola B, Walther TC, and Ferguson SM (2012). The transcription factor TFEB links mTORC1 signaling to transcriptional control of lysosome homeostasis. Sci. Signal. 5, ra42. 10.1126/scisignal.2002790. [PubMed: 22692423]

67. Feng WW, Bang S, Takacs EM, Day C, Crawford KJ, Al-Sheyab R, Almufarrej DB, Wells W, Ilchenko S, Kasumov T, et al. (2023). Hepatic Huwe1 loss protects mice from non-alcoholic fatty liver disease through lipid metabolic rewiring. iScience 26, 108405. 10.1016/j.isci.2023.108405. [PubMed: 38047073]

68. Sahu U, Villa E, Reczek CR, Zhao Z, O'Hara BP, Torno MD, Mishra R, Shannon WD, Asara JM, Gao P, et al. (2024). Pyrimidines maintain mitochondrial pyruvate oxidation to support de novo lipogenesis. Science 383, 1484–1492. 10.1126/science.adh2771. [PubMed: 38547260]

69. Peterson TR, Sengupta SS, Harris TE, Carmack AE, Kang SA, Balderas E, Guertin DA, Madden KL, Carpenter AE, Finck BN, and Sabatini DM (2011). mTOR complex 1 regulates lipin 1 localization to control the SREBP pathway. Cell 146, 408–420. 10.1016/j.cell.2011.06.034. [PubMed: 21816276]

70. Porstmann T, Santos CR, Griffiths B, Cully M, Wu M, Leevers S, Griffiths JR, Chung YL, and Schulze A (2008). SREBP activity is regulated by mTORC1 and contributes to Akt-dependent cell growth. Cell Metab. 8, 224–236. 10.1016/j.cmet.2008.07.007. [PubMed: 18762023]

71. Yoshida S, Hong S, Suzuki T, Nada S, Mannan AM, Wang J, Okada M, Guan KL, and Inoki K (2011). Redox regulates mammalian target of rapamycin complex 1 (mTORC1) activity by modulating the TSC1/TSC2-Rheb GTPase pathway. J. Biol. Chem. 286, 32651–32660. 10.1074/jbc.M111.238014. [PubMed: 21784859]

72. Sakasai-Sakai A, Takata T, Takino JI, and Takeuchi M (2017). Impact of intracellular glyceraldehyde-derived advanced glycation end-products on human hepatocyte cell death. Sci. Rep. 7, 14282. 10.1038/s41598-017-14711-3. [PubMed: 29079763]

73. Hao Z, Duncan GS, Su YW, Li WY, Silvester J, Hong C, You H, Brenner D, Gorrini C, Haight J, et al. (2012). The E3 ubiquitin ligase Mule acts through the ATM-p53 axis to maintain B lymphocyte homeostasis. J. Exp. Med. 209, 173–186. 10.1084/jem.20111363. [PubMed: 22213803]

74. Postic C, Shiota M, Niswender KD, Jetton TL, Chen Y, Moates JM, Shelton KD, Lindner J, Cherrington AD, and Magnuson MA (1999). Dual roles for glucokinase in glucose homeostasis as determined by liver and pancreatic beta cell-specific gene knock-outs using Cre recombinase. J. Biol. Chem. 274, 305–315. 10.1074/jbc.274.1.305. [PubMed: 9867845]

75. Sarbassov DD, Guertin DA, Ali SM, and Sabatini DM (2005). Phosphorylation and regulation of Akt/PKB by the rictor-mTOR complex. Science 307, 1098–1101. 10.1126/science.1106148. [PubMed: 15718470]

76. Sanjana NE, Shalem O, and Zhang F (2014). Improved vectors and genome-wide libraries for CRISPR screening. Nat. Methods 11, 783–784. 10.1038/nmeth.3047. [PubMed: 25075903]

77. Kamitani T, Kito K, Nguyen HP, and Yeh ET (1997). Characterization of NEDD8, a developmentally down-regulated ubiquitin-like protein. J. Biol. Chem. 272, 28557–28562. 10.1074/jbc.272.45.28557. [PubMed: 9353319]

78. Inoue S, Hao Z, Elia AJ, Cescon D, Zhou L, Silvester J, Snow B, Harris IS, Sasaki M, Li WY, et al. (2013). Mule/Huwe1/Arf-BP1 suppresses Ras-driven tumorigenesis by preventing c-Myc/Miz1-mediated down-regulation of p21 and p15. Genes Dev. 27, 1101–1114. 10.1101/gad.214577.113. [PubMed: 23699408]

79. Chaanine AH, Higgins L, Markowski T, Harman J, Kachman M, Burant C, Navar LG, Busija D, and Delafontaine P (2021). Multi-Omics Approach Profiling Metabolic Remodeling in Early Systolic Dysfunction and in Overt Systolic Heart Failure. Int. J. Mol. Sci. 23, 235. 10.3390/ijms23010235. [PubMed: 35008662]

Highlights

- HUWE1 and CAD preferentially interact with ubiquitinated Rheb
- HUWE1 further ubiquitinates Rheb and supports Rheb interaction with mTORC1 and CAD
- HUWE1 stimulates mTORC1 activity through its E3 ligase activity
- HUWE1 also supports pyrimidine synthesis by enhancing CAD expression

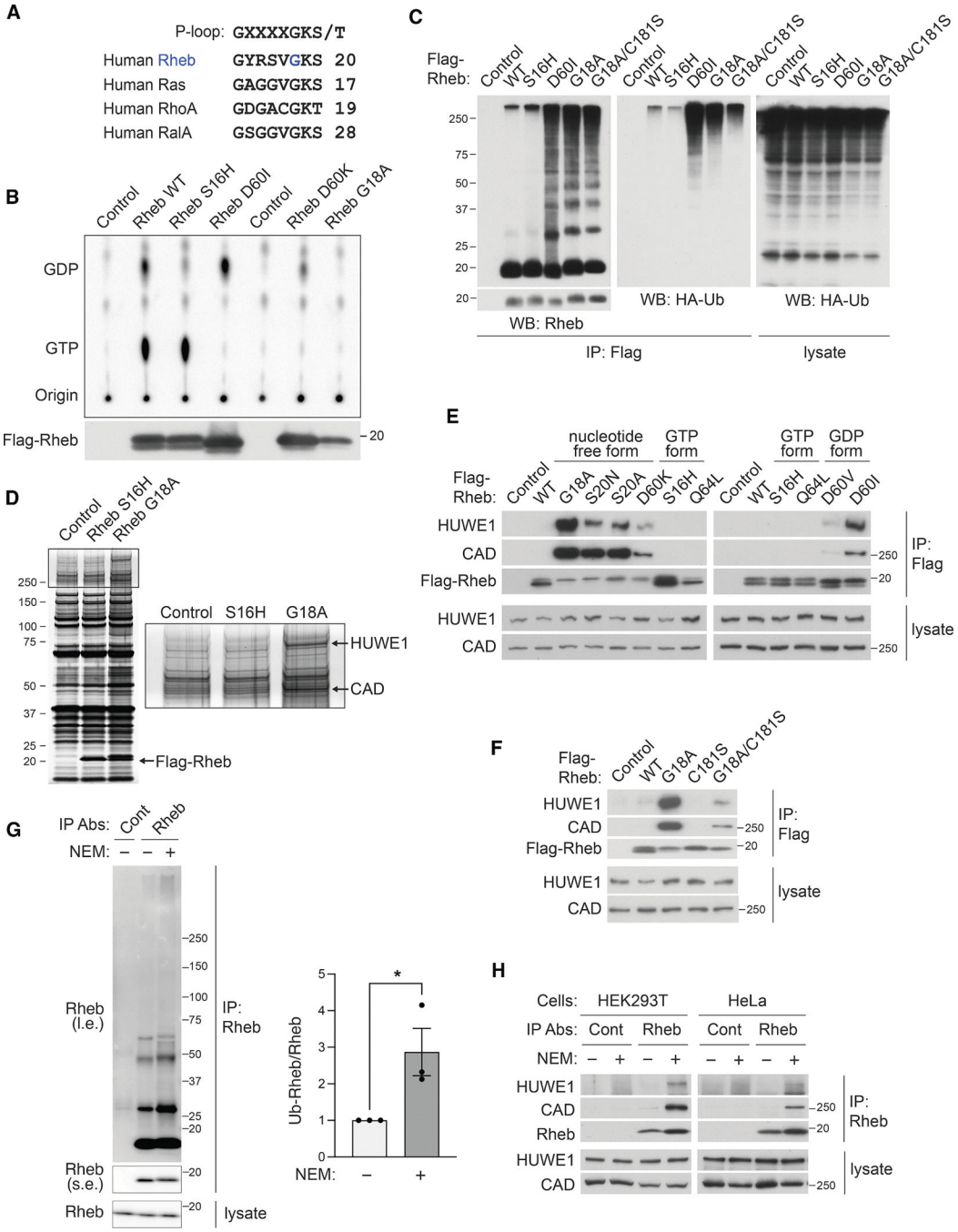

Figure 1. The ubiquitinated nucleotide-free or GDP-bound form of Rheb preferentially interacts with endogenous HUWE1 and CAD

(A) The GXXXXGKS/T domain (P loop) is conserved in the Ras family of small GTPases. Rheb has a conserved Gly18 residue (blue).

(B) G18A mutation leads to nucleotide dissociation from Rheb. HEK293T cells transiently expressing the indicated Rheb mutants were labeled with ^{32}P orthophosphate. The levels of GTP and GDP bound to the IPed FLAG-Rheb were determined.

(C) Nucleotide-free and GDP-bound form of Rheb mutants are highly ubiquitinated. HEK293T cells were co-transfected with HA-Ub and the indicated FLAG-Rheb constructs.

FLAG-Rheb was IPed, and levels of high-molecular-weight Rhebs were monitored by Rheb or HA antibody. A short exposure of the non-ubiquitinated Rheb blot was included in the left panel.

(D) Highly ubiquitinated nucleotide-free Rheb G18A mutant strongly interacts with endogenous HUWE1 and CAD. HEK293T cells were transfected with FLAG-Rheb S16H or G18A mutant. FLAG-Rheb was IPed, and coIPed proteins were visualized by silver staining and followed by mass spectrometry analyses.

(E) Nucleotide-free or GDP-bound form of Rheb preferentially interacts with endogenous HUWE1 and CAD. The indicated FLAG-Rhebs were IPed, and co-IPed endogenous HUWE1 and CAD were monitored.

(F) Blocking membrane tethering of Rheb G18A mutant mitigates its interaction with HUWE1 and CAD. The C181S mutation was introduced in wild-type Rheb and the G18A Rheb mutant. The experiments were performed as in (1E).

(G) Inhibition of DUB activity maintains levels of ubiquitinated endogenous Rheb. Endogenous Rheb was IPed in the lysis buffer without or with NEM (100 mM), and the levels of ubiquitinated Rheb were monitored. Quantification was expressed as the ratio of Ub-Rheb to non-Ub-Rheb. $*p < 0.05$, mean ± SEM, $n = 3$. s.e. and l.e. indicate short and long exposure, respectively.

(H) Inhibition of DUB activity increases interaction between endogenous Rheb and HUWE1 or CAD. The interaction between endogenous Rheb and HUWE1 was monitored in the presence or absence of NEM (100 mM) in the lysates from HEK293T or HeLa cells.

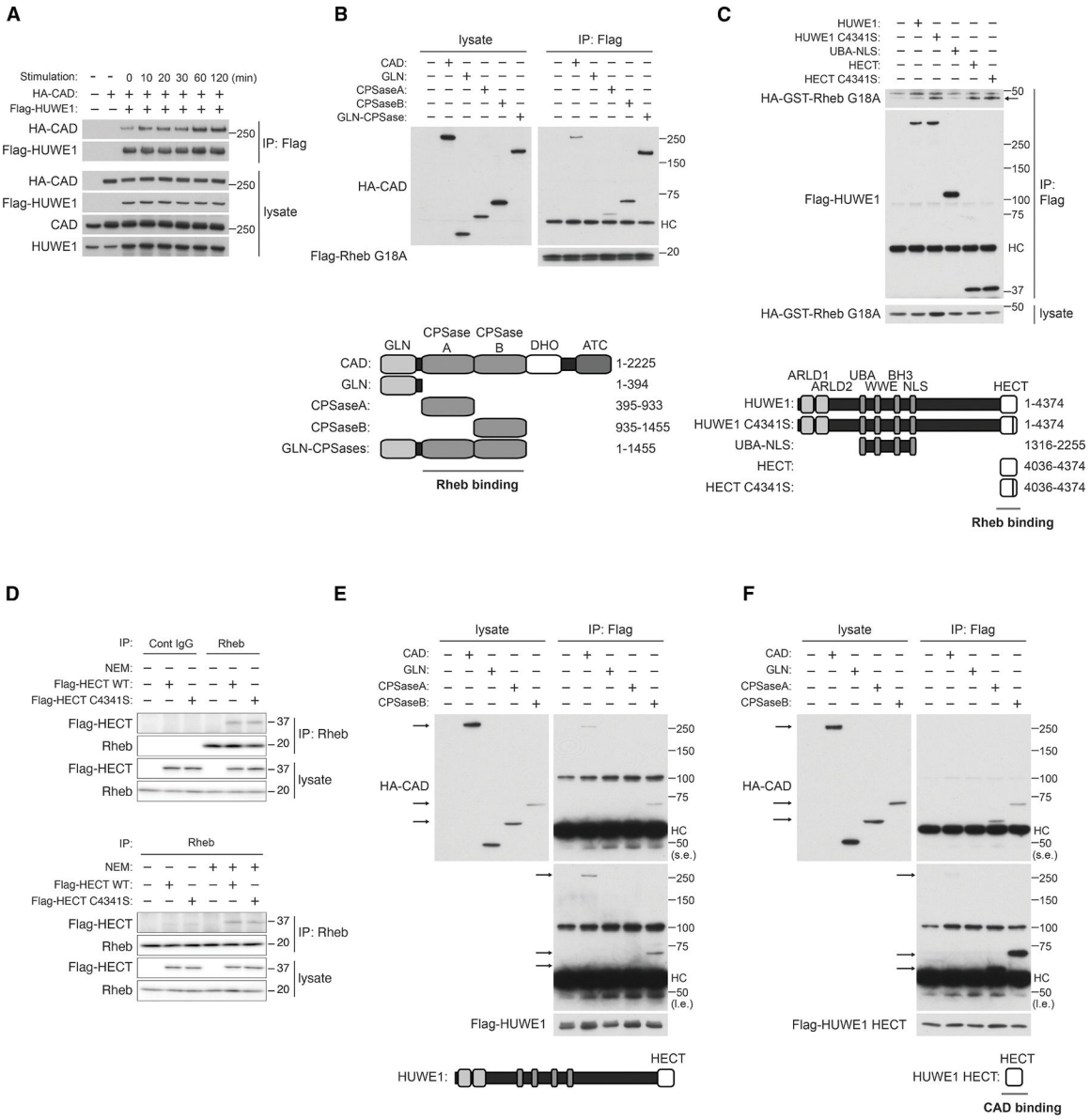

Figure 2. Characterization of binding modules of Rheb-HUWE1-CAD interaction

(A) HUWE1 interacts with CAD. HEK293T cells transiently expressing HA-CAD and FLAG-HUWE1 were starved with Hank's Balanced Saline (HBSS) and then stimulated with DMEM containing 10% fetal bovine serum (FBS). FLAG-HUWE1 was IPed, and levels of coIPed HA-CAD were monitored.

(B) The Rheb G18A mutant interacts with the CPSase domain of CAD. HEK293T cells expressing FLAG-Rheb G18A and the indicated HA-CAD and HA-CAD fragments were lysed and IPed with FLAG-beads. coIPed HA-CAD was monitored. HC denotes IgG heavy chain.

(C) The Rheb G18A mutant interacts with the HECT domain of HUWE1. HEK293T cells expressing the indicated FLAG-HUWE1 and FLAG-HUWE1 fragments and HA-GST-Rheb G18A were lysed and IPed with FLAG-beads. coIPed HA-GST-Rheb G18A was monitored. The arrow indicates coIPed Rheb.

(D) Inhibition of DUB activity increases interaction between endogenous Rheb and the HECT domain of HUWE1. Endogenous Rheb was IPed, and levels of coIPed HECT-domain of HUWE1 were determined in the presence or absence of NEM in the lysates from HEK293T cells.

(E and F) HUWE1 and its HECT domain interact with the CPSase domain of CAD. HEK293T cells expressing FLAG-HUWE1 (E) or FLAG-HUWE1-HECT (F) with the indicated HA-CAD and HA-CAD fragments were lysed and IPed with FLAG-beads. coIPed HA-CAD was monitored. The arrows indicate coIPed CAD fragments.

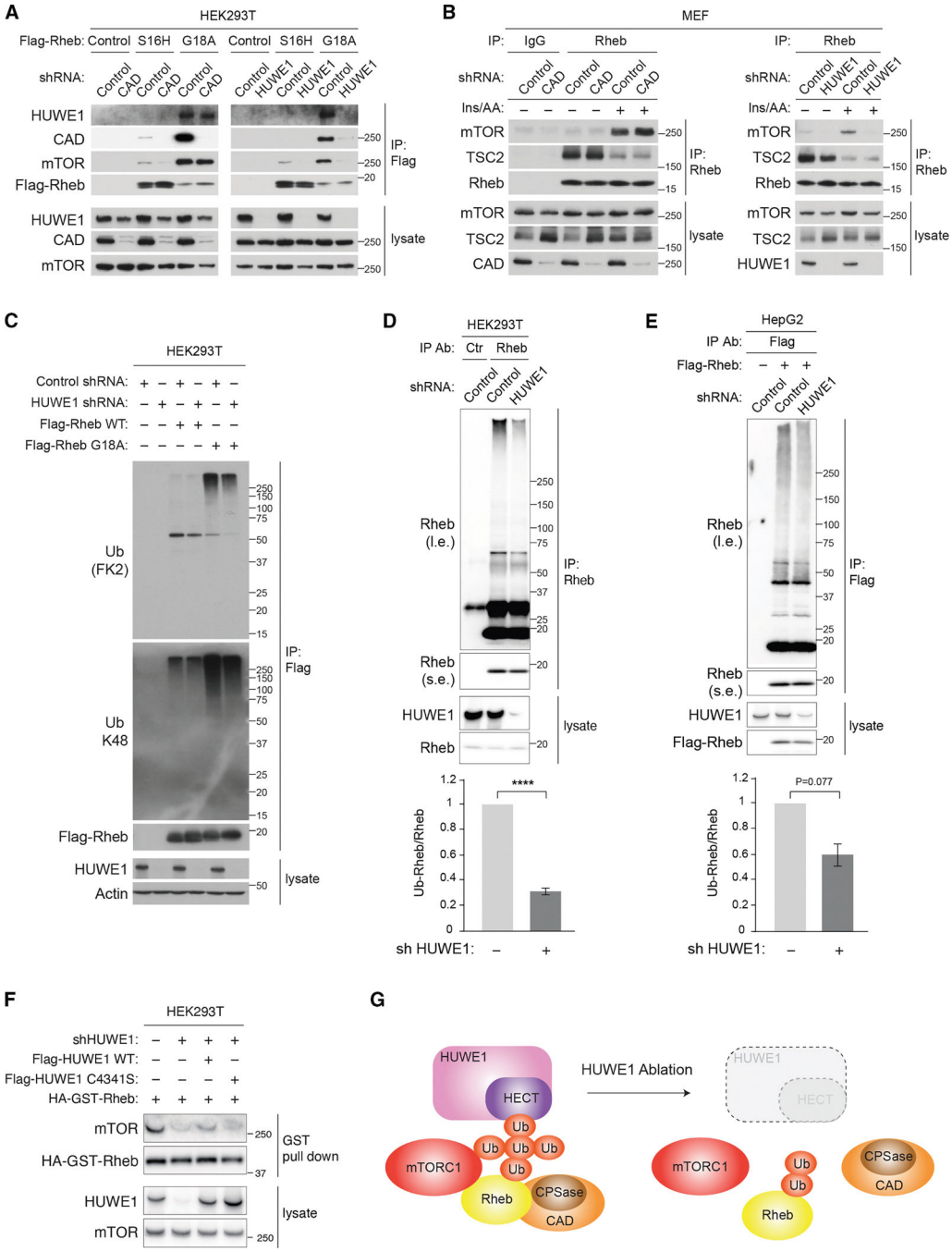

Figure 3. HUWE1 is required for Rheb to interact with CAD and mTOR

(A) HUWE1 is required for the Rheb G18A mutant to interact with CAD and mTOR. HEK293T cells expressing control, HUWE1, or CAD shRNA were transfected with the FLAG-Rheb S16H or FLAG-Rheb G18A mutant. FLAG-Rhebs were IPed, and levels of coIPed endogenous HUWE1, CAD, and mTOR were monitored.

(B) HUWE1, but not CAD, is required for endogenous Rheb to interact with mTOR. Endogenous Rheb was IPed from MEFs expressing control, CAD, or HUWE1 shRNA

under *in vivo* crosslinking conditions. Levels of coIPed endogenous mTOR and TSC2 were monitored.

(C) Ablation of HUWE1 decreases Rheb ubiquitination. HUWE1 is knocked down with the shRNA in HEK293T cells expressing FLAG-tagged wild-type Rheb and G18A Rheb mutant. Levels of ubiquitinated Rheb were monitored using pan-ubiquitin (FK2) or K48-linked ubiquitin antibodies.

(D and E) Ablation of HUWE1 decreases endogenous Rheb ubiquitination. HUWE1 is knocked down with the shRNA in HEK293T cells (D) and HepG2 cells (E). Levels of ubiquitinated endogenous Rheb (Ub-Rheb) were monitored. Quantification was displayed as a ratio of Ub-Rheb/non-Ub-Rheb. ****$p < 0.0001$, mean ± SEM, $n = 3$ (D) and $p = 0.0768$, mean ± SEM, $n = 3$ (E). Note that the KD efficiency of HUWE1 in HepG2 cells was low.

(F) The E3 ligase activity of HUWE1 is required for Rheb to interact with mTOR. HEK293T cells ablated HUWE1 were transiently transfected with HA-GST-Rheb and FLAG-HUWE1 or FLAG-HUWE1 C4341S mutant. Cell lysates were subjected to a GST pull-down assay, and the levels of endogenous mTOR co-precipitated with HA-GST-Rheb were monitored.

(G) Hypothetical model of HUWE1 function in forming Ub-Rheb-mTORC1-CAD complex. The HECT domain of HUWE1, which recognizes its substrates and ubiquitinated residues, and the CPSase domain of CAD are required for the interactions between HUWE1, CAD, and Rheb. The ablation of HUWE1 or its ubiquitin ligase activity disrupts the interaction between Rheb and mTOR or CAD. These observations suggest that HUWE1 plays a critical role in enhancing Rheb to interact with both mTORC1 and CAD, possibly through Rheb ubiquitin modification.

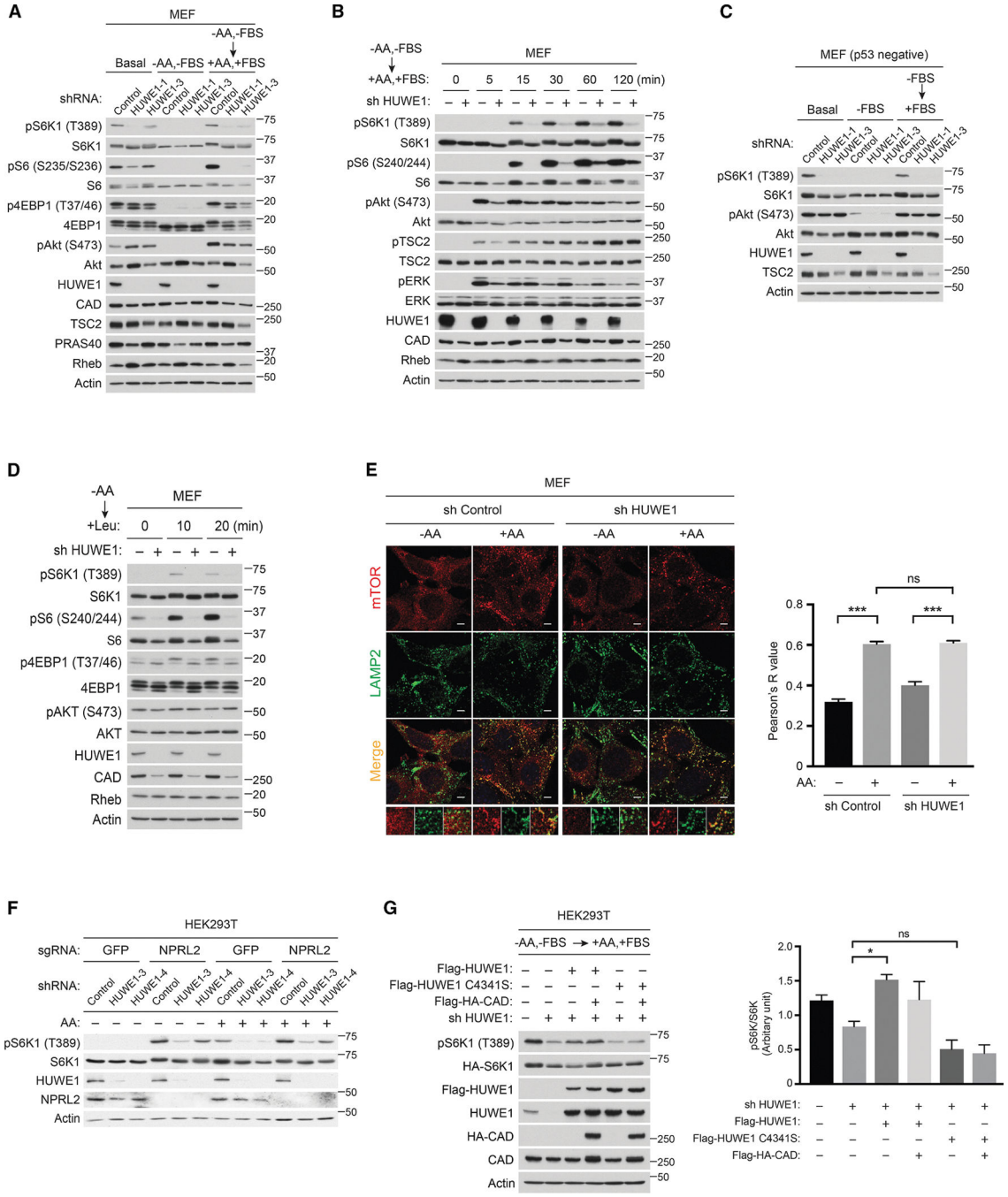

Figure 4. HUWE1 enhances mTORC1 activity

(A) HUWE1 is required for growth factor/amino acid-induced mTORC1 activation. MEFs were infected with control (scramble) or two distinct HUWE1 shRNAs, and levels of mTORC1 and mTORC2 activity and the indicated protein expression were monitored under steady-state culture (basal), HBSS starved (1 h, HBSS), or growth factor/amino acid-stimulated (20 min, DMEM containing 10% FBS) conditions.

(B) KD of HUWE1 delays and reduces growth factor/amino acid-induced mTORC1 activation (time course). MEFs expressing HUWE1 shRNA were starved with HBSS for 60 min and then stimulated with DMEM containing 10% FBS for the indicated times.
(C) HUWE1 promotes growth factor-induced mTORC1 activation independent of p53. MEFs derived from a p53 null embryo were infected with control or two distinct HUWE1 shRNAs, and levels of mTORC1 and mTORC2 activity were monitored.
(D) HUWE1 is required for amino acid-induced mTORC1 activation. MEFs were infected with HUWE1 shRNA, and the levels of the indicated protein expression were monitored under leucine-starved (50 min) or leucine-stimulated (10 or 20 min) conditions.
(E) HUWE1 is dispensable for amino acid-induced lysosomal mTOR localization. MEFs expressing control or HUWE1 shRNA were amino acid-starved for 50 min and then stimulated with 1× amino acids for 10 min. Double IF staining with mTOR (red) and LAMP2 (green) antibodies was performed. Pearson's correlation coefficient, R value, was determined for quantifying the colocalization of mTOR and LAMP2 and graphed as a $***p < 0.001$, ns (not significant), mean ± SEM, $n = 28$ (sh control, −AA), $n = 38$ (sh control, +AA), $n = 23$ (sh HUWE1, −AA), and $n = 29$ (sh HUWE1, +AA). Scale bars, 10 μm.
(F) Ablation of HUWE1 inhibits mTORC1 activity in cells lacking NPRL2 expression. HUWE1 was ablated in control and NPRL2 KO HEK293T cells using two distinct shRNAs, and the effect of amino acid-induced mTORC1 activation was determined.
(G) The E3 ligase activity of HUWE1 is required for mTORC1 activation. HEK293T cells ablated endogenous HUWE1 were transiently transfected with FLAG-HUWE1 or the catalytically inactive FLAG-HUWE1 C4341S mutant in the presence or absence of HA-CAD with HA-S6K1 as a reporter. Cells were starved for 60 min and stimulated with DMEM containing 10% FBS for 60 min. Levels of pS6K1/HA-S6K1 were quantified (right graph). Data were expressed as $*p < 0.05$, mean ± SEM, $n = 3$.

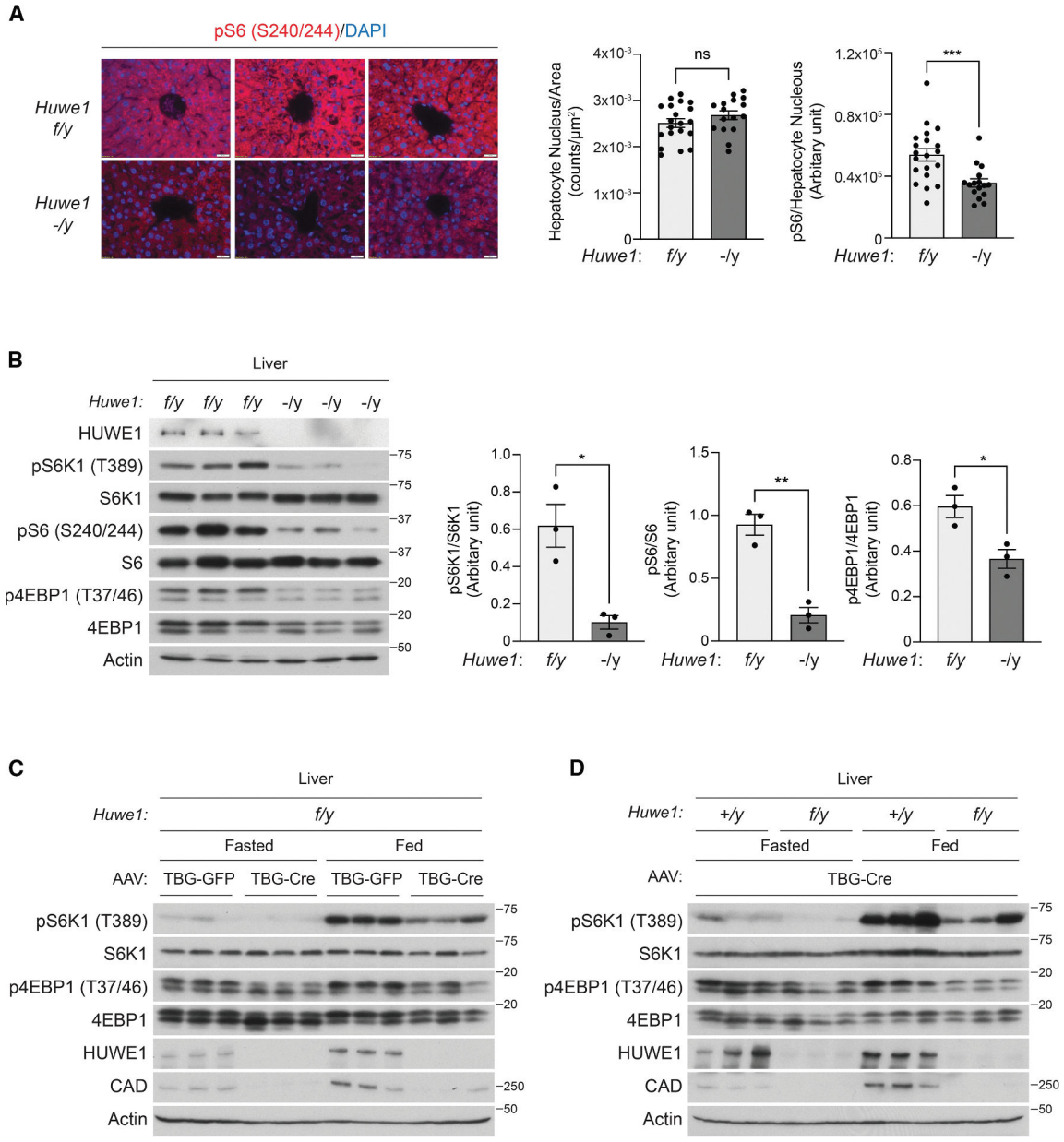

Figure 5. HUWE1 supports mTORC1 activity in the murine liver tissues

(A and B) Congenital ablation of HUWE1 in hepatocytes reduced the mTORC1 activity in the murine liver tissues. Male control (*Huwe1*$^{f/y}$) and *Huwe1 LKO* (*Huwe1*$^{-/y}$) mice (12-week-old) were starved for 16 h and fed for 5 h. The mTORC1 activity and nucleus number of liver tissues (right posterior segment VI) were monitored by staining with pS6 (S240/S244) antibody and DAPI. Quantification was demonstrated as the nucleus number of hepatocytes/area (counts/μm^2) and the intensity of pS6/nucleus number of hepatocytes (arbitrary unit). ***$p < 0.001$, mean ± SEM, $n = 16$–20 images, Scale bars, 20 μm (A). Levels of mTORC1 activity were determined by immunoblot of the liver lysates. Quantification was demonstrated as a ratio of the phosphorylated protein/total protein, *$p <$ 0.05 and **$p < 0.01$, mean ± SEM, $n = 3$ (B).

(C and D) Inducible ablation of HUWE1 in hepatocytes suppresses mTORC1 activity in the adult murine liver tissues under fasted and fed conditions. AAV-TBG-Cre or AAV-TBG-GFP (control) was administered into *Huwe1*$^{f/y}$ male mice (12-week-old) via the tail vein (C). AAV-TBG-Cre was administered into control (*Huwe1*$^{+/y}$) or *Huwe1*$^{f/y}$ mice (D). Levels of mTORC1 activity and the indicated protein expression in the liver tissues were monitored.

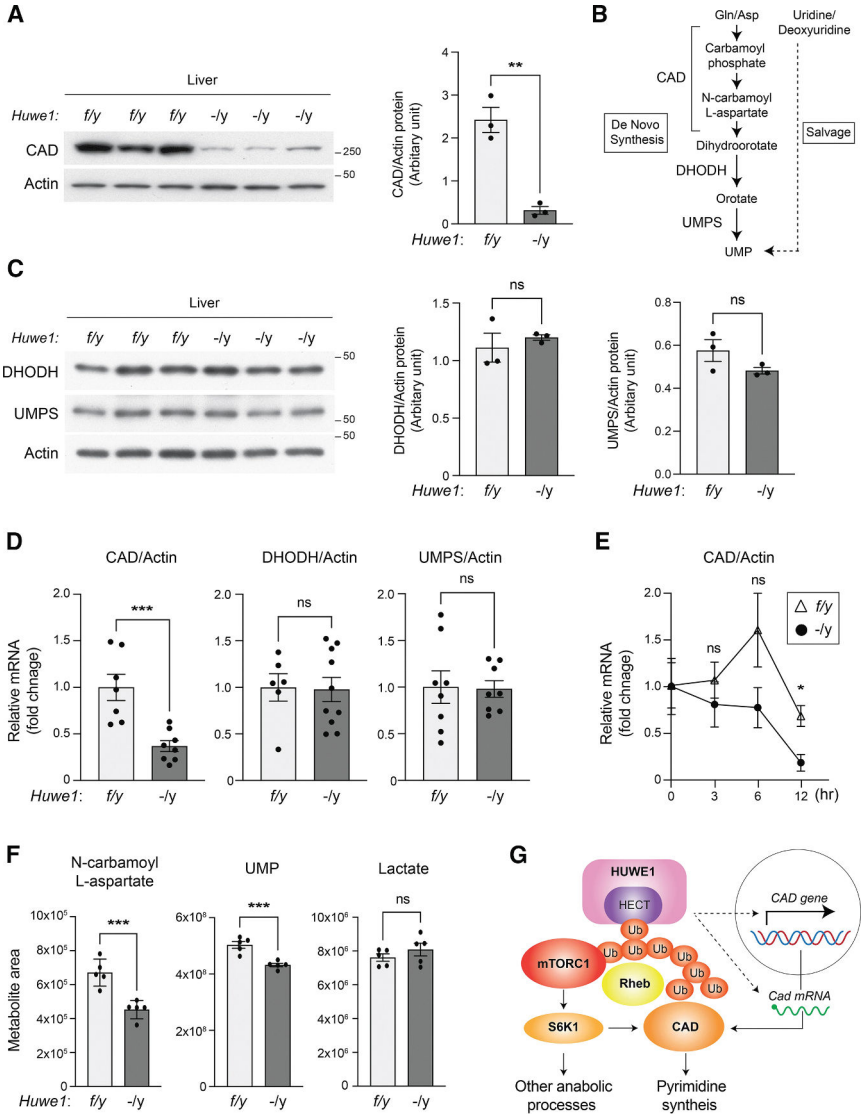

Figure 6. HUWE1 supports *de novo* pyrimidine synthesis by maintaining CAD expression

(A) HUWE1 is required for maintaining CAD protein expression in liver tissues. Levels of CAD protein expression were determined in *Huwe1 LKO* (*Huw*$^{-/y}$) and control (*Huwe1*$^{f/y}$) liver tissues. Experiments were performed as in Figure 5A. Quantification of CAD protein was expressed as a ratio of CAD/Actin, $^{**}p < 0.01$, mean ± SEM, $n = 3$.

(B) Scheme of *de novo* and salvage pyrimidine synthesis pathways. CAD catalyzes the first three steps of *de novo* pyrimidine synthesis and generates intermediate metabolites, carbamoyl phosphate, N-carbamoyl-L-aspartate, and dihydroorotate.

(C) HUWE1 KO does not affect the levels of DHODH and UMPS in the liver tissues. Levels of DHODH and UMPS protein expression were determined in *Huwe1 LKO* (*Huwe1*$^{-/y}$) and control (*Huwe1*$^{f/y}$) liver tissues. Quantification of the proteins was expressed as a ratio of DHODH/actin or UMPS/actin, mean ± SEM, $n = 3$.

(D) HUWE1 KO specifically reduces the levels of CAD mRNA in the liver tissues. Levels of CAD, DHODH, and UMPS mRNA were determined in the liver tissues of the indicated

mice. Data were expressed as a ratio of the indicated mRNA/actin, ***$p < 0.001$, mean ± SEM, $n = 6–10$.

(E) HUWE1 maintains the stability of CAD mRNA. Primary cultured hepatocytes were obtained from *Huwe1 LKO* (*Huwe1*$^{-/y}$) and control (*Huwe1*$^{f/y}$) liver tissues. Levels of CAD mRNA were determined by qPCR after the indicated time of treatment with actinomycin D (1 μg/mL). Data were expressed as a ratio of CAD/actin, *$p < 0.05$, mean ± SEM, $n = 3$.

(F) The ablation of HUWE1 reduced the levels of N-carbamoyl-L-aspartate and UMP in the liver tissues. Levels of N-carbamoyl-L-aspartate, UMP, and lactate were determined in the *Huwe1 LKO* (*Huwe1*$^{-/y}$) and control (*Huwe1*$^{f/y}$) liver tissues by mass spectrometry analyses. ***$p < 0.001$, mean ± SEM, $n = 5$.

(G) The hypothetical model for HUWE1-dependent regulation of mTORC1 activity and *de novo* pyrimidine synthesis. Both HUWE1 and CAD preferentially interact with ubiquitinated Rheb. HUWE1-dependent modification of Ub-Rheb may play key roles in supporting Rheb-mTORC1 interaction and subsequent mTORC1-S6K1 activation, leading to CAD activation. Simultaneously, HUWE1 increases levels of CAD mRNA and maintains CAD protein expression, as well as *de novo* pyrimidine synthesis.

KEY RESOURCES TABLE

REAGENT or RESOURCE	SOURCE	IDENTIFIER
Antibodies		
Rabbit polyclonal anti-p-S6K1 T389	Cell Signaling Technology	Cat#9205; RRID:AB_330944
Rabbit monoclonal anti-S6K1 (49D7)	Cell Signaling Technology	Cat#2708; RRID:AB_390722
Rabbit monoclonal anti-p-4EBP1 Thr37/46 (236B4)	Cell Signaling Technology	Cat#2855; RRID:AB_560835
Rabbit monoclonal anti-4EBP1 (53H11)	Cell Signaling Technology	Cat#9644; RRID:AB_2097841
Rabbit polyclonal anti-p-S6 S240/244	Cell Signaling Technology	Cat#2215; RRID:AB_331682
Rabbit monoclonal anti-p-S6 S235/236 (2F9)	Cell Signaling Technology	Cat#4856; RRID:AB_2181037
Rabbit monoclonal anti-S6 (5G10)	Cell Signaling Technology	Cat#2217; RRID:AB_331355
Rabbit monoclonal anti-*p*-Akt S473 (193H12)	Cell Signaling Technology	Cat#4058; RRID:AB_331168
Rabbit polyclonal anti-Akt	Cell Signaling Technology	Cat#9272; RRID:AB_329827
Rabbit monoclonal anti-*p*-TSC2 T1462 (5B12)	Cell Signaling Technology	Cat#3617; RRID:AB_490956
Rabbit monoclonal ant-TSC2 (D93F12)	Cell Signaling Technology	Cat#4308; RRID:AB_10547134
Rabbit monoclonal anti-p-p44/42 MAPK T202/Y204 (20G11)	Cell Signaling Technology	Cat#4376; RRID:AB_331772
Rabbit monoclonal anti-p44/42 MAPK (137F5)	Cell Signaling Technology	Cat#4695; RRID:AB_390779
Rabbit polyclonal anti-PRAS40	Cell Signaling Technology	Cat#2610; RRID:AB_916206
Rabbit monoclonal anti-Rheb (E1G1R) (for IP and WB)	Cell Signaling Technology	Cat#13879; RRID:AB_2721022
Rabbit monoclonal anti-mTOR (7C10) (for IF and WB)	Cell Signaling Technology	Cat#2983; RRID:AB_2105622
Rabbit monoclonal anti-Rab9 (D22A6)	Cell Signaling Technology	Cat#5133; RRID:AB_10634754
Rabbit polyclonal anti-NPM1	Cell Signaling Technology	Cat#3542; RRID:AB_2155178
Mouse monoclonal anti-Rheb (M01) (for IF and WB)	Abnova	Cat#H00006009-M01; RRID:AB_1112097
Rabbit polyclonal anti-Lasu1/Ureb1 (WB)	Bethyl Laboratories	Cat#A300-486A; RRID:AB_2264590
Rabbit polyclonal anti-HUWE1 (for IF)	Millipore Sigma	Cat#AHPA002548; RRID:AB_1080489
Rabbit polyclonal anti-HUWE1 (for WB)	Novus	Cat#NB100-652; RRID:AB_2264587
Rabbit polyclonal anti-CAD (for IP and WB)	Thermo Fisher Scientific	Cat#A301-372A; RRID:AB_2798079
Rabbit polyclonal anti-CAD (for WB)	Cell Signaling Technology	Cat#11933; RRID:AB_279777
Mouse monoclonal anti-beta Actin (AC15)	Sigma-Aldrich	Cat#A1978; RRID:AB_476692
Mouse monoclonal anti-beta Actin (8H10D10)	Cell Signaling Technology	Cat#3700; RRID:AB_2242334
Rabbit monoclonal anti-K48-linkage specific polyubiquitin (D9D5)	Cell Signaling Technology	Cat#8081; RRID:AB_1085989
Rabbit monoclonal anti-K63-linkage specific polyubiquitin (HWA4C4)	Enzo Biochem	Cat#BML-PW0600-0025; RRID: AB_2052278
Rabbit polyclonal anti-DHODH	Proteintech	Cat#14877-1-AP; RRID:AB_2091723
Rabbit polyclonal anti-UMPS	Proteintech	Cat#14830-1-AP; RRID:AB_2212392
Mouse monoclonal anti-Rheb (clone 2C11) (for WB)	Novus Biologicals	Cat#H00006009-M01; RRID:AB_1112097
Rabbit polyclonal anti-GST	Novus Biologicals	Cat#NB600-326; RRID:AB_10001229
Rabbit polyclonal anti-LAMP1	Abcam	Cat#ab24170; RRID:AB_775978
Mouse monoclonal anti-LAMP2 (clone H4B4)	Abcam	Cat#ab25631; RRID:AB_470709
Mouse monoclonal anti-Flag (clone M2)	Sigma-Aldrich	Cat#1804; RRID:AB_262044

REAGENT or RESOURCE	SOURCE	IDENTIFIER
Mouse monoclonal anti-FLAG®M2 Affinity Gel	Sigma-Aldrich	Cat#A2220; RRID:AB_10063035
Mouse monoclonal anti-*c*-Myc (clone 9E10)	Covance	Cat#MMS-150P-500; RRID:AB_291324
Mouse monoclonal anti-HA (clone 16B12)	Covance	Cat#MMS-101R; RRID:AB_291262
Mouse monoclonal anti-ubiquitinylated proteins (FK2)	MilliporeSigma	Cat#04–263; RRID:AB_612093
Alexa Fluor 594-goat polyclonal anti-rabbit IgG	Thermo Fisher Scientific	Cat#A11012; RRID:AB_141359
Alexa Fluor 488-goat polyclonal anti-mouse IgG	Thermo Fisher Scientific	Cat#A11029; RRID:AB_138404
Alexa Fluor 594-goat polyclonal anti-mouse IgG	Thermo Fisher Scientific	Cat#R37121; RRID:AB_2556549
Anti-rabbit IgG HRP-Linked Whole Ab	GE Healthcare	Cat#NA934; RRID:AB_772206
Anti-mouse IgG HRP-Linked Whole Ab	GE Healthcare	Cat#NA931; RRID:AB_772210
Bacterial and virus strains		
One Shot™ Stbl™ Chemically Competent E. coli	Thermo Fisher Scientific	Cat#C737303
Chemicals, peptides, and recombinant proteins		
Amino acid mixtures	Sigma-Aldrich	Cat#R7131
L-Glutathione reduced	Sigma-Aldrich	Cat#G4251
N-Ethylmaleimide (NEM)	Sigma-Aldrich	Cat#E3876
Saponin	Sigma-Aldrich	Cat#S4521
Actinomycin D	Sigma-Aldrich	Cat#A9415
Lipofectamine 3000	Invitrogen	Cat#L3000001
Amino acid-free DMEM medium	US Biological Life Sciences	Cat#D9800-27
Leucine-free DMEM medium	Crystalgen	Cat#226-024
L-leucine	RPI	Cat#L22000
Dialyzed Fetal Bovine Serum	Thermo Fisher Scientific	Cat#26400044
Pierce™ Glutathione Agarose	Thermo Fisher Scientific	Cat#16100
Prolong Gold antifade reagent with DAPI	Thermo Fisher Scientific	Cat#P36931
Protein G Sepharose 4 Fast Flow	GE Healthcare	Cat#17061801
Flag peptide	LifeTein	Cat#LT12022
Insulin	Sigma-Aldrich	Cat#10908
Phosphorus-32	NEN Radiochemicals	Cat#NEX011
MgATP Solution	R&D Systems	Cat#B-20
Critical commercial assays		
Subcellular Protein Fractionation Kit	Thermo Fisher Scientific	Cat#78840
TriFECTa RNAi Kits	Integrated DNA Technologies (IDT)	N/A
Experimental models: Cell lines		
Human: HEK293T	ATCC	Cat#CRL-3216
Human: HeLa	Yoshida et al.[71]	N/A
Human: HepG2	Sakasai-Sakai et al.[72]	N/A
Mouse: embryonic fibroblasts	Yoshida et al.[71]	N/A

REAGENT or RESOURCE	SOURCE	IDENTIFIER
Mouse: embryonic fibroblasts *p53*$^{-/-}$	Dr. David J Kwiatkowski[46]	N/A
Experimental models: Organisms/strains		
B6.129P2(Cg)-*Huwe1*$^{tm1.1Mak}$/J	The Jaxon Laboratory Hao et al.[73]	Strain#029254; RRID:IMSR_JAX:029254
B6.Cg-*Speer6-ps1*$^{Tg(Alb-cre)21Mgn}$/J	The Jaxon Laboratory Postic et al.[74]	Strain#003574; RRID:IMSR_JAX:003574
Oligonucleotides		
shRNA targeting HUWE1-1 (H and M) 5′-GCATCTGTACAGTTCCATAGA	This paper	N/A
shRNA targeting HUWE1-2 (H and M) 5′-TGCCGCAATCCAGACATAT	This paper	N/A
shRNA targeting HUWE1-3 (H and M) 5′-GCTCAATACTAGCCGTCTACA	This paper	N/A
shRNA targeting HUWE1-4 (H) 5′-GGGAATTTCCCACCAGGATGA	This paper	N/A
sgRNA targeting HUWE1 (H) 5′-GCTGAACTTCACCTGAATCG	This paper	N/A
sgRNA targeting GFP 5′-CTTGTCACTACTTTCGGTTA	Yao et al.[20]	N/A
shRNA targeting CAD-1 (M) 5′-GCTCAGATCCTAGTGCTAACG	This paper	N/A
shRNA targeting CAD-2 (M) 5′-GGTGGTGATGGACATCTATGA	This paper	N/A
siRNA sequences for HUWE1, see Table S1	Integrated DNA Technologies (IDT)	N/A
RT-qPCR primer sequences, see Table S2	This paper	N/A
Recombinant DNA		
pLKO1-Sc (Scramble shRNA)	Sarbassov et al.[75]	Addgene plasmid #1864
Lenti-CRISPR v2	Sanjana et al.[76]	Addgene plasmid #52961
psPAX2	Dr. Didier Trono	Addgene plasmid #12260
pMD2.G	Dr. Didier Trono	Addgene plasmid #12259
pcDNA3-HA-Ubiquitin	Kamitani et al.[77]	Addgene plasmid #18712
pcDNA3-Flag-HA-CAD	Ben-Sahra et al.[31]	Addgene plasmid #46238
pENTR1A-HUWE1	Dr. Jeanette G Cook	Addgene plasmid #37431
pENTR1A-HUWE1 C4341S	Dr. Jeanette G Cook	Addgene plasmid #37432
pRK7-Flag-human Rheb	This paper	N/A
pRK7-Flag-human Rheb C181S	This paper	N/A
pRK7-Flag-human Rheb S16H	This paper	N/A
pRK7-Flag-human Rheb G18A	This paper	N/A
pRK7-Flag-human Rheb G18A C181S	This paper	N/A
pRK7-Flag-human Rheb S20N	This paper	N/A
pRK7-Flag-human Rheb S20A	This paper	N/A
pRK7-Flag-human Rheb D60K	This paper	N/A

REAGENT or RESOURCE	SOURCE	IDENTIFIER
pRK7-Flag-human Rheb D60I	This paper	N/A
pRK7-Flag-human Rheb Q64L	This paper	N/A
pRK5-HA-GST-human Rheb	This paper	N/A
pcDNA3-Flag-CAD	This paper	N/A
pcDNA3-HA-CAD	This paper	N/A
pcDNA3-HA-CAD GLN	This paper	N/A
pcDNA3-HA-CAD CPSase A	This paper	N/A
pcDNA3-HA-CAD CPSase B	This paper	N/A
pcDNA3-HA-CAD GLN CPSase	This paper	N/A
pRK7-Flag-HUWE1	This paper	N/A
pRK7-Flag-HUWE1 C4341S	This paper	N/A
pRK7-Flag-HUWE1 UBA-NLS	This paper	N/A
pRK7-Flag-HUWE1 HECT	This paper	N/A
pRK7-Flag-HUWE1 HECT C4341S	This paper	N/A
pGEX-KG-GST-Rheb	Inoki et al.[10]	N/A
AAV-TBG-GFP	This paper	N/A
AAV-TBG-Cre	This paper	N/A
Software and algorithms		
ImageJ	NIH	https://imagej.nih.gov/ij/
GraphPad Prism 8	GraphPad	https://www.graphpad.com/scientific-software/prism/
Adobe Photoshop CS6	Adobe	https://www.adobe.com/products/photoshop.html
Adobe Illustrator 2023	Adobe	https://www.adobe.com/products/illustrator.html
Deposited Data		
Mendeley Data (Blots, Immunofluorescence)	This paper	https://data.mendeley.com/preview/snppdxjf2s, https://doi.org/10.17632/snppdxjf2s.1